ABSTRACT

RACHAEL ELANA JEANETTE MCCAULLY. Sources and Variability of Nitrate on an Alaskan Hillslope Dominated by Alder Shrubs (Under the direction of Dr. Carli Arendt).

In Arctic ecosystems, feedbacks exist between vegetation, nutrient availability, and permafrost. Increasing temperatures are driving the expansion of nitrogen (N) fixing shrubs and increasing available nitrate (NO_3^-), a critical limiting nutrient across tundra landscapes. Alder shrubs (*alnus fruticosa*), which contain N-fixing bacteria, may be a major control on NO_3^- availability in the Arctic, along with microtopographically driven soil moisture and permafrost degradation. Understanding how vegetation and nutrient availability will continue to shift in the face of global climate change is crucial to inform future Earth System Models (ESMs), yet many details about these systems remain unknown. The purpose of this study was to identify and constrain the spatiotemporal variability of NO_3^- in an alder dominated permafrost landscape. The chemical composition of soil pore water was investigated on a hillslope in the Seward Peninsula, Alaska, USA, during the early and late growing seasons of 2017 and 2018. Soil pore water was collected from upslope, within, and downslope of alder patches growing on a steep, well-drained hillslope and analyzed for anion and cation concentrations as well as stable isotopic composition of NO_3^- ($\delta^{15}N$ and $\delta^{18}O$) and water ($\delta^{18}O$ and δD). The primary findings of this study are that soil pore water NO_3^- varied significantly on multiple spatial (within and between alder patches) and temporal (daily and seasonally) scales within the alder dominated permafrost landscape we investigated. Spatially, NO_3^- from locations within alder patches had elevated NO_3^- concentrations of up to 58 mg L^{-1} and were significantly different from upslope (0.11 ± 0.25 mg L^{-1}) and downslope concentrations (0.10 ± 0.06 mg L^{-1}). Isotopic analysis ($\delta^{15}N$ and $\delta^{18}O$) confirmed that our measured NO_3^- was a product of microbial degradation of N-rich alder shrub organic matter, as well as minor sources of organic matter. Dynamic temporal variation in NO_3^-

within and downslope of alder patches correspond to precipitation events, where NO_3^- likely accumulated in the soil and was flushed downslope during rainfall. Finally, enrichment of both $\delta^{15}N$ and $\delta^{18}O$ at wetter downslope locations indicates that denitrification buffers the mobility and spatial extent of NO_3^-. These findings have important implications for degrading permafrost systems of the Arctic where newly developed hydrologic pathways have the potential to increase the mobility of nutrients. Furthermore, this study indicates that interactions between NO_3^-, shrubs, permafrost, and topography are complicated and further investigation is needed to fully understand climate feedbacks as permafrost landscapes respond to a warming Arctic.

Sources and Variability of Nitrate on an Alaskan Hillslope Dominated by Alder Shrubs

by
Rachael Elana Jeanette McCaully

A thesis submitted to the Graduate Faculty of
North Carolina State University
in partial fulfillment of the
requirements for the degree of
Master of Science

Marine, Earth, and Atmospheric Sciences

Raleigh, North Carolina
2019

APPROVED BY:

Dr. Carli A. Arendt Committee Chair	Dr. Brent D. Newman External Member
Dr. Dean Hesterberg	Dr. David Genereux

BIOGRAPHY

I was raised in Waxhaw, North Carolina and received a Bachelor of Arts in Earth Sciences and Geology from the University of North Carolina at Charlotte in 2014. Upon completion of my undergraduate career I moved to Raleigh, NC, where I worked for Wake County Environmental Services for the next three years. During this time I became a licensed Environmental Health Specialist and gained valuable experience working as a public servant and learning about environmental regulations at the state and local levels. I returned to academia in May 2017 when I became a student intern at Los Alamos National Laboratory (LANL) in New Mexico. While there I was able to collaborate with scientists at the federal government level and participate in an innovative research project sponsored by the Department of Energy, called Next Generation Ecosystem Experiments (NGEE) Arctic. In August of 2017 I began the Master's program in the Marine, Earth, and Atmospheric Sciences Department at NCSU and continued on in close collaboration with NGEE Arctic. This thesis is a result of the field and lab work made possible by support from NGEE Arctic and LANL.

ACKNOWLEDGMENTS

This research was completed with oversight and support of the Next-Generation Ecosystems Experiments (NGEE Arctic) project. NGEE Arctic is supported by the Office of Biological and Environmental Research in the U.S. Department of Energy – Office of Science. I would like to thank Carli A. Arendt for investing in my success as an early career scientist and for her unwavering support. I would like to thank Brent Newman and Jeff Heikoop for their invaluable knowledge and guidance pertaining to isotope geochemistry in Arctic systems. I would like to thank Sanna Sevanto, Nathan Wales, Verity Salmon, Nate Conroy, Emma Lathrop, Oana Marina, George Perkins, Emily Kluk, and Dea Musa for their assistance in fieldwork, laboratory, and manuscript preparation. I would like to thank Bob Busey for access to continuous weather data. Thank you to Cathy Wilson, Stan Wullshleger, and the entire NGEE Arctic team for their support. I would like to thank Ethan Hyland and Gwen Hopper for laboratory assistance in the Department of Marine, Earth, and Atmospheric Science at North Carolina State University, and William Showers for the use of sampling equipment. Finally, thank you to my husband and partner Patrick McCaully for supporting me and encouraging me to pursue a career in science.

TABLE OF CONTENTS

LIST OF TABLES

LIST OF FIGURES

1.0. INTRODUCTION

1.1. Background

Ecosystems in the Arctic are directly and continually impacted by the effects of increasing global temperatures (Martin *et al.*, 2009, Chapin *et al.*, 2000, Hovelsrud *et al.*, 2011), yet many details remain unknown about how vegetation and nutrient availability in permafrost systems will shift in response to climate change (Sharkhuu & Sharkhuu, 2012; Keuper *et al.*, 2017; Barnes *et al.*, 2014). Due to rising temperatures and longer growing seasons, the Arctic is experiencing permafrost degradation with subsequent feedbacks that impact soil moisture, vegetation, and nutrient availability (Weintraub & Schimel, 2005; Hinzman *et al.*, 2013; Wavoord & Kurylyk, 2016). Hydrologic conditions and nutrient transport in the Arctic are controlled by the seasonal freezing and thawing of permafrost in the upper soil layer, known as the active layer (Boike *et al.*, 2018).

Continuous permafrost soils are commonly saturated with limited vertical drainage where the average thickness of the active layer above the permafrost remains relatively constant on an inter-annual basis (Atchley *et al.*, 2016). Prolonged warming of permafrost allows for the development of interconnected vertical drainage pathways from increased melt that bisect previously uninterrupted/continuous permafrost (Bense *et al.*, 2009; Minsley *et al.*, 2012; Walvoord *et al.*, 2012), resulting in well-drained, drier soils (Woo *et al.*, 2008). In addition to altering tundra hydrology, permafrost degradation (Romanovsky & Osterkamp, 2000) also alters landscape biogeochemistry including the carbon cycle.

Permafrost acts as a substantial storage reservoir for frozen carbon-based organic material. The carbon (C) stored within the top 3 m of soil in the northern circumpolar permafrost region is estimated to be 1,035 ± 150 Pg C (Hugelius *et al.*, 2014; Schuur *et al.*, 2015). Increased

microbial decomposition of organic matter associated with warmer soils triggers the release of C formerly stored within frozen soil (Weintraub & Schimel, 2005; Schuur *et al.*, 2008; Keuper *et al.*, 2012; Schuur *et al.*, 2008). This C may be sequestered in biomass or released into the atmosphere as methane (CH_4) or carbon dioxide (CO_2) (Schädel *et al.*, 2016). As permafrost degrades, increased thickness of the active soil layer, thawing of previously frozen organic matter, and newly created hydrologic pathways alter nutrient production and mobility. Deeper active layers can result in the growth and expansion of larger plant functional types (including shrubs) that require drier soils and deeper thaw to accommodate their root systems (Myers-Smith *et al.*, 2011). The phenomenon of shrubs increasing in density and abundance in permafrost landscapes, is known as 'shrub expansion' or 'shrubification' (Tape, Sturm, & Racine, 2006).

Certain shrub species are more closely associated with climate-induced shrubification than others. *Alnus fruticosa* (green alder) is one of those species (Myers-Smith *et al.*, 2011), which are woody shrubs that fix atmospheric nitrogen (N_2) through the symbiotic relationship with microbes residing within nodules in the alder root systems (Roy *et al.*, 2007). Alders frequently establish on steep hillslopes with degraded or discontinuous permafrost (Myers-Smith *et al.*, 2011), and have been associated with elevated concentrations of nitrate (NO_3^-) in soil pore water in permafrost at high elevations like the Alps (Bühlmann *et al.*, 2016; Hiltbrunner *et al.*, 2014).

Shrubification may lead to increased C storage within new biomass, promoting a negative climate feedback (Euskirchen *et al.*, 2016). However, Mack *et al.*, (2004) found that the amount of C that is mobilized and released from the degradation of previously frozen soils is substantially greater than the amount of C storage potential in new plant growth. Previous and ongoing research demonstrates the linkages that exist between N and C in arctic tundra

(Weintraub & Schimel, 2003; McClelland *et al.*, 2007; Koch *et al.*, 2013; Street, Burns, & Woodin, 2015) and the importance of understanding both cycles. In Arctic tundra ecosystems, N is a critical controlling nutrient (Shaver & Chapin, 1980) where ammonium (NH_4), and NO_3^- are typically significantly limited. Organic and inorganic N can be introduced to soil through lateral inputs, N_2 fixation, atmospheric deposition, animal inputs, and melting permafrost (Keuper *et al.*, 2017).

Increased NO_3^- availability as a result of shifts in plant functional type has implications that extend to neighboring ecosystems. Inputs of NO_3^- from upland areas into surface waters can impact downslope hydrochemistry and alter downstream ecosystems by promoting the growth of NO_3^- adaptive vegetation and decreasing biodiversity (Vitousek *et al.*, 1997; Hiltbrunner, 2014). The mobility potential of nutrients across the permafrost landscape is largely dependent on topographic gradient, which also influences vegetation, drainage, and soil redox environments (Ogawa *et al*., 2006; O'Donnell & Jones, 2006). However, previous studies have determined that more research is needed to constrain N-fixing vegetation and topographic controls on NO_3^- mobility in the Arctic (Harms & Ludwig, 2016).

The effects of alder on soil chemistry and stream water chemistry are well documented. Hurd & Raynel (2004) found elevated subsurface and stream water NO_3^- in a riparian wetland dominated by alders in the Adirondack Mountains, and a study in the Swiss Alps measured elevated soil pore water NO_3^--N (Bühlmann *et al.*, 2016). Two independent studies on the Kenai Peninsula of Alaska found that alder cover explained 75-95% of the variation of NO_x-N (nitrate-nitrite) in 25 streams (Shaftel *et al*., 2010), and significantly greater stream bank interstitial concentrations of ammonium and nitrate + nitrite existed in watersheds with alder than those without (Whigham *et al.*, 2017). Mitchell & Ruess (2009) determined that alders contributed

fixed-N to soil in a post-fire upland area of interior AK with no permafrost. In permafrost soils of northwest AK, alders were found to influence soil NO_3^-, and high foliar N in various plant types growing under within alder understory suggested increased soil N below the shrubs (Rhoades *et al.*, 2001). While the linkage between alders and soil N is clear (Hurd & Raynel, 2004; Bühlmann *et al.*, 2016; Shaftel *et al.*, 2010; Whigham *et al.*, 2017; Mitchell & Ruess, 2009; Rhoades *et al.*, 2001), the spatial and temporal variability of soil pore water NO_3^- in relation to alders, topography, and permafrost in the Arctic has not previously been studied in detail.

1.2. Study Objectives

This study was conducted as part of Next Generation Ecosystem Experiments - Arctic (NGEE - Arctic), a Department of Energy (DOE) project that informs Earth System Models (ESM) through the collection and incorporation of experimental data in the face of Arctic climate change. We investigate the relationships that exist between N-fixing alders, topography, and soil moisture to determine the dominant controls on NO_3^- production and availability that occur in permafrost soils on a hillslope landscape. We hypothesize that at our Kougarok Hillslope study location (Figure 1): 1) alders are the dominant source of NO_3^- to soil pore water through mineralization and nitrification of organic matter derived from alder leaf litter and woody material; 2) NO_3^- availability varies both spatially (within individual patches and from one patch to another) and temporally (daily and seasonally) across permafrost landscapes; and 3) NO_3^- mobility is buffered by changes in redox conditions across the hillslope topographic gradient.

1.3. Location

Approximately 80 km north of the Alaskan coastal town of Nome and 12 km east of Mary's Igloo, the research hillslope of interest is located at mile marker 64 of Kougarok Road (65.160714 N, -164.828275 W) and is referred to as the Kougarok Hillslope (KG Hillslope;

Figure 1). KG Hillslope is a prominent hillslope of moderate relief with shallow metamorphic (schist) bedrock and permafrost. The hill slopes steeply (19.2%) towards Kuzitrin River to the north and west, and gently (8.7%) towards a series of shallow thermokarst lakes to the east. The KG Hillslope has well drained mineral soils with an organic peat horizon and leaf litter on the soil surface (taxanomic soil classification not available), and vegetation found on the KG Hillslope includes densely populated *Alnus viridus* spp. *fruticosa* (hereafter referred to as alder) patches, moss and lichen, and microshrub (Salmon *et al.*, In Prep.; Iversen *et al.*, 2016). As the slope breaks onto a lower gradient toe slope (referred to as 'KG Toe Slope'), vegetation shifts into a tussock tundra savannah with sedge, moss, lichen, and intermittent shrubs. Soils on the KG Toe Slope are deeper than on the KG Hillslope, have a thicker organic horizon, and are constrained by continuous permafrost and therefore poorly drained. These soils are frequently saturated in inter-tussock areas.

A recent study estimated that alder area coverage on the KG hillslope increased by 40% from 7.4 ha in 1956 to 10.4 ha in 2014, with an average rate of alder shrubland expansion of 513 m^2 yr^{-1} (Salmon *et al.*, In Prep.). For our study, soils within and in close proximity to five alder patches were initially examined around the perimeter of the KG Hillslope, and later two of the five patches of interest underwent additional monitoring.

2.0. METHODS

To investigate the aforementioned hypotheses, this study was subdivided into two phases: an initial phase to identify NO_3^- 'hotspots' in relation to alder (Phase 1) and a comprehensive informed phase (Phase 2) to further address each of the three hypotheses. Phase 1 (July 18-21, 2017) consisted of a synoptic survey to establish soil NO_3^- variability in proximity to five alder

patches located on the hillslope study site. Sampling locations were placed upslope (US), within (WI), and downslope (DS) of five alder patches (A1-A5) in July 2017. Two transects were established along the Eastern slope of the KG Toe Slope: 1) a Road Transect that was parallel to and ~5 m from the road, and 2) a Middle Transect that was 400 m upslope of and parallel to the road transect (locations shown in Figure 1a). Phase 2 (September 14-16, 2017, July 22-27, 2018 and September 21-22, 2018) addresses the spatiotemporal variability of NO_3^- within (located on the KG Hillslope) and downslope (located on the KG Toe Slope) of two of the five alder patches that were exposed to the same topographic and climatic conditions and examines this variability with respect to topographic gradient. These two patches are located at similar relief on the east facing KG Hillslope, however they exist separately from one another, allowing the nutrient dynamics associated with one patch to be examined independently from the other. These alder patches were examined with increasing spatial and temporal resolution throughout sampling campaigns to determine NO_3^- variability within a single patch and to capture the extent of NO_3^- availability down gradient of each patch. To address these controls, we measured soil pore water NO_3^- concentrations within and surrounding alder patches, and employed a dual isotope method using $\delta^{15}N\text{-}NO_3^-$ and $\delta^{18}O\text{-}NO_3^-$ to determine sources of NO_3^- and biogeochemical processes such as denitrification occurring in soil pore water across alder shrub tundra.

Soil pore water and bulk soil were collected from each sampling location to assess NO_3^- concentrations and soil moisture. In July 2017, the A2, A3, A4, A5, Middle transect, and Road transect locations were sampled only once while the A1 locations were sampled daily for four days to capture variations in NO_3^- variability (n = 34). In September 2017, upslope, within, and downslope locations of both A1 and A4 were sampled once daily for the duration of a three-day sampling campaign (n = 28). A1 is roughly ~3,400 m^2 in area and located 20 m north of A4,

which is ~6,400 m^2 in area (Figure 1a, 1b). In July and September of 2018, samples were collected every 10 m along transects initiating within A1 and A4 and terminating 50 m downslope from the bottom of each patch (Figure 1b). Samples were collected daily for five days (n = 123) in July 2018 and once in September 2018 (n = 40).

2.1. Soil Pore Water

Soil pore water samples were collected by installing macro-rhizons (Rhizosphere Research Products; hereby referred to as rhizons) using the methods described by Seeberg-Elverfeldt (2005). Rhizons, which have a porous tip through which water can pass free of ion exchange, were installed at depths between 15-30 cm, and due to the volume required for chemical analyses, were installed in nests (on average 5 rhizons per nest) at each sampling location depending on soil saturation and water availability. Soil pore water was collected in 60 ml syringes connected to luar locks on each rhizon, which were subsequently combined into one sample per nest to obtain adequate volumes for analyses and ensure a homogenous bulk sample. Samples were immediately filtered with a 1.5 μm pre-filter and a 0.45 μm filter and stored in HDPE Nalgene bottles for major cation and anion analysis. Anion samples were frozen and cation samples were preserved to a pH < 2 with nitric acid and frozen. Syringes were re-hung from rhizons at their respective sampling locations and left overnight before collection the next day. Soil pore water samples were transported to Los Alamos National Laboratory's Geochemistry and Geomaterials Research Laboratory (GGRL) where they were stored frozen until analysis.

Cations were measured using inductively coupled plasma optical emission spectrometry (OES) using United States Environmental Protection Agency (EPA) methods 200.7. Anions were measured with ion chromatography utilizing EPA method 300 (Throckmorton *et al*., 2015);

precision is justified to 0.01 mg L^{-1}. Ammonium (NH_4^+) concentrations were determined for a subset of samples (n = 92) with the phenolhypochlorite method (Cary 100 Bio UV-Visible Spectrophotometer). Isotopic data for $\delta^{15}N$ and $\delta^{18}O$ of NO_3^- were measured using the methods outlined in Heikoop *et al.,* (2015), where a modified denitrifier method outlined by Sigman *et al.*, (2001) and Casciotti *et al.,* (2002) using a GV Isoprime isotope ratio mass spectrometer (IRMS) coupled to a TraceGas peripheral instrument. Isotopic data for $\delta^{18}O$ - H_20 was measured using a GV Instruments Multiflow peripheral instrument coupled to a GV Isoprime IRMS (Heikoop *et al.*, 2015). Isotope values of nitrate and water are reported in delta (δ) notation in parts per thousand (‰) as the deviation from a standard of known composition, atmospheric N_2 for NO_3^- and VSMOW (Vienna Standard Mean Ocean Water) for water.

2.2. Soil and leaf litter

At each sampling location, soil was collected for soil moisture analysis from 15 cm depths (and at 30 cm depths where soil was deep enough) in pre-weighed tins, sealed with parafilm, and frozen for preservation. One to two soil tins were collected for every sampling location. Pebbles, roots, and leaf litter were removed from the tins upon collection to avoid any mass bias. A total of 27 soil samples were collected during July 2017, 6 during September 2017, and 24 in July 2018.

In July 2018, three soil pits (P1, P2, and P3) were dug and described along the A1 downslope transect (Figure 1). In each pit, soil was excavated to frozen soil, verified by presence of ice and sub-freezing soil temperatures. Soil was collected at an interval of 20 cm in each pit. Pits 2 and 3 had total depths of 46 cm and 55 cm to frozen soil, respectively, and soil samples were collected at 20 cm and 40 cm. Pit 1 had a depth of 61 cm to frozen soil and soil samples were collected at 20 cm, 40 cm, and 60 cm depths.

All soil samples were frozen and transported to GGRL and North Carolina State University Department of Marine, Earth, and Atmospheric Sciences in Raleigh, North Carolina where they were stored frozen until analysis. Gravimetric soil moisture was measured where soil and tins were weighed, dried at 80° C for a minimum of 72 hours, and reweighed. Soil moisture was determined as the difference in mass between wet and dry soil. After the soil was dried, chemical analyses were performed on the soil including total N and $\delta^{15}N$ of soil organic nitrogen (SON). Thirteen soil samples and leaf litter from five locations within A1 and A4 collected in September 2018 were analyzed for total N, $\delta^{15}N$ of soil organic nitrogen (SON) and C/N ratios using a Costech Elemental Analyzer coupled to a Thermo Delta V IRMS. Leaf litter was collected in September 2018 from five locations within A1 and A4. Litter was stored in sealed plastic bags frozen, and homogenized prior to analysis.

2.3. In-field parameters

In-situ parameters were measured for each water sample and include depth to frozen soil or bedrock, soil temperature, soil pore water pH, dissolved oxygen, and specific conductivity. A 1 m steel frost probe was used to measure the depth (cm) to frozen soil, roots, or bedrock at each location, which were sampled once in July 2017, daily in September 2017, and twice in July 2018. Depths were averaged from three measurements per rhizon nest. Soil temperature was measured in tandem with soil depth measurements using an Orion thermometer. An Orion pH meter and YSI multi-parameter meter were used to collect *in situ* hydrochemistry parameters in unfiltered samples upon collection. Dissolved oxygen was measured in July 2017 and 2018 using a Hach Portable Optical DO Probe or YSI multi-parameter meter. Iron (Fe) speciation parameters were collected during the July 2018 field campaign for two days, which were mixed with ferrozine on-site and later analyzed at GGRL using the Fe-ferrozine method. The Fe

speciation method determined Fe^{2+} and total Fe (Fe_{Total}) (Stookey, 1970). Fe^{3+} was later calculated as the difference between Fe^{2+} and Fe_{Total}.

2.4. Statistical Analysis

Nonparametric Mann-Whitney rank sum tests were performed (Helsel & Hirsch, 2002) to identify significant differences between NO_3^- concentrations at locations within and outside of alder patches in Phase 1, and within and downslope of A1 and A4 in Phase 2. These rank sum tests were also used for Fe_{Total} in Phase 2. P-values less than 0.05 are considered statistically significant. General linear regressions were used to determine relationships between variables including NO_3^-, soil moisture, depth to frozen soil or bedrock, and Fe. Coefficient of variability (Brown, 1998) was calculated for calcium (Ca), sodium (Na), chloride (Cl^-), and NO_3^- by dividing the standard deviation of the population by the population mean in order to directly compare the variability within each chemical compound across the KG field site. MATLAB R2017a was used for all statistical analyses and figure generation.

3.0. RESULTS

Phase 1 includes synoptic survey results and preliminary hydrochemistry data demonstrating that soil pore water within alder patches contains heterogeneous, elevated concentrations of NO_3^-. Phase 2 assesses spatial and temporal variations in NO_3^- during three separate field campaigns within two patches on the KG Hillslope, as well as the mobility of NO_3^- down gradient with respect to topography. Of n = 92 samples measured for ammonium (NH_4^+), only 16 had concentrations above 0.02 mg L^{-1}, 38 had concentrations < 0.01 mg L^{-1} and all but one (0.29 mg L^{-1}) measured ammonium (NH_4^+) concentrations were < 0.1 mg L^{-1}. Therefore, although likely an important intermediate form of nitrogen, NH_4^+ was not considered a

significant source of inorganic N in this study (Table 1). Lastly, pH, DO, and conductivity were recorded during sampling but no direct correlations with NO_3^- were observed. Summaries of pH, DO, and conductivity are provided in Table 2, however these parameters are not discussed in depth within this study.

3.1. Soil Depth and Moisture

3.1.1. Phase 1 Soil Conditions

Soils within each patch are similar in composition with general defining characteristics of a surficial peat horizon underlain by organic material (decayed peat) and a transitional horizon into mineral soil. During Phase 1, the mean depth to bedrock or frozen soil was 35.2 ± 2.9 cm on the KG Hillslope (including 'within' and 'upslope' locations) and 29.4 ± 3.0 cm on the KG Toe Slope (Table 3). Mean soil moisture content (percent dry/wet weight) ranged from 28.5 ± 20.9 % on the KG Hillslope to 55.9 ± 23.8 % on the KG Toe Slope. While soil pore water NO_3^- was elevated on the well-drained KG Hillslope and negligible on the poorly-drained KG Toe Slope, no direct correlation between NO_3^- and soil moisture was identified ($r^2 = 0.0127$; Figure 2).

3.1.2. Phase 2 Soil Conditions

During September 2017 sampling (September 14-16) the KG Toe Slope was saturated with standing water in the inter-tussock areas. Mean soil moisture on the KG Hillslope was 28.4 ± 14.2 %. Mean depth to rock or frozen soil was 43.6 ± 21.7 cm on the KG Hillslope and 56.5 ± 5.4 cm on the KG Toe Slope. In July 2018 (July 22-27), the mean soil moisture on the KG Hillslope was 36.7 ±14.9 % and 51.0 ± 22.7 % on the KG Toe Slope, and mean depth to bedrock or frozen soil increased from 36.6 ± 7.3 cm on the KG Hillslope to 53.3 ±12.1 cm on the KG Toe Slope along the A1 and A4 50 m transects (Table 3). Soil moisture content and depth to bedrock

or frozen soil were not measured or recorded during September 2018 (September 21-22) sampling.

3.2. Phase 1: Synoptic results from five alder patches

3.2.1. July 2017

From July 18-21 soil pore water NO_3^- was elevated (> 1.0 mg L^{-1}) within A1, A2, A3, and A5 (Figure 3). Atmospheric conditions were mild (~13° C) and dry for three out of the four sampling days (brief precipitation event overnight on July 18th; Western Regional Climate Center, 2017). NO_3^- within A1 on 18 July had a concentration of 0.52 mg L^{-1} and increased by more than an order of magnitude on July 19th (8.29 mg L^{-1}) and maintained concentrations between 8-10 mg L^{-1} through July 20th and 21st (Figure 4). A similar increase was also observed at a seep in the hillslope down gradient of A1 on 19 July relative to all other sampling days. This seep is likely representative of active layer melt flowing directly from A1 to the toe slope (Figure 1b), perhaps through fractured bedrock. Soil pore water within A4 had NO_3^- concentrations of < 1.0 mg L^1 in July 2017. All sample locations upslope of the A1-A5 alder patches had low NO_3^- soil pore water concentrations (< 1.0 mg L^{-1}). Phase 1 results show that soil pore water NO_3^- was elevated within alder patches. The four-day sample collection within A1 revealed daily variations in NO_3^- (0.51 to 10.08 mg L^{-1}). Both the Road and the Middle transects on the toe slope downslope of A1 and A4 had low NO_3^- (< 1.0 mg L^{-1}).

3.3. Phase 2: NO_3^- variability between two alder patches

3.3.1. September 2017

During the 2017 September sampling campaign (September 14-16), conditions were cool (~5.4° C) and wet, with daily precipitation (direct observation; Western Regional Climate Center, 2017). A1 and A4 were examined in greater detail by increasing the spatial resolution of

soil pore water chemistry (Figure 1b). NO_3^- was elevated within A4 and downslope of A1, the latter of which increased daily from 1.46 mg L^{-1} on September 14 to 5.49 mg L^{-1} on September 16 (Figure 4, Table 4). Soil pore water samples from the KG Hillslope between A1 and A4 had negligible NO_3^- (< 0.01 mg L^{-1}). Nitrate concentrations did not vary significantly between locations within and directly downslope of A1 and A4 (Table 5; $p > 0.05$), however the mean of these two locations did differ significantly ($p < 0.05$) from the Middle and Road transects lower on the KG Toe Slope.

3.3.2. July 2018

During the 2018 July sampling campaign (July 22-27), NO_3^- was elevated in A1 (4.57 to 6.52 mg L^{-1}) and A4 (2.08 to 5.73 mg L^{-1}) at locations within each alder patch and up to 20 m downslope of each alder patch (Figure 5). Each of the five sampling days in July were dry with no precipitation (~16° C), and slight temporal variation (< 3 mg L^{-1}) in NO_3^- was observed in some locations. NO_3^- concentrations measured from two soil pits along the A1 transect also increased with depth, from 3.57 mg L^{-1} at 20 cm depth to 8.32 mg L^{-1} at 60 cm depth in Pit 1 and 6.52 mg L^{-1} at 20 cm depth to 7.59 mg L^{-1} at 40 cm depth in Pit 3. However, Pit 2 had negligible NO_3^- (0.03 ± 0.02 mg L^{-1}).

Nitrate decreased from 5.73 mg L^{-1} (single value) within A4 to 0.02 ± 0.02 mg L^{-1} on the downslope A4 transect (Figure 6b; Table 6) and from 6.52 ± 1.24 mg L^{-1} within A1 to 0.02 ± 0.01 mg L^{-1} on the downslope A1 transect. The transition between elevated NO_3^- towards low or negligible NO_3^- was observed between 0-10 m downslope of A4, and between 0-30 m downslope of A1. Manganese (Mn) increased from 0.02 mg L^{-1} (single value) within A4 to 0.32 ± 0.05 mg L^{-1} along the A4 downslope transect and Fe^{2+} ranged from 0.32 ± 0.03 mg L^{-1} to 5.21 ± 3.05 mg L^{-1} (Figure 6b and Figure 7; Table 6), respectively. Sulfate (SO_4^{2-}) ranged from 1.83 mg L^{-1} (single value) to 0.52 ± 0.23 mg L^{-1} (Figure 6b; Table 6). Spatial trends were not identified in

concentrations of Mn, Fe^{2+} and SO_4^{2-} within or downslope of A1 (Figure 6a, Table 6) with respect to reducing zones.

3.3.3. September 2018

In September 2018 (21-22), similar patterns in NO_3^- concentration occurred along both A1 and A4 transects (Table 7), with the highest NO_3^- (17.73 mg L^{-1} in A1 and 8.44 mg L^{-1} in A4) at locations within and directly downslope of alders. Total Fe increased along the A4 transect (0.11 mg L^{-1} to 17.07 mg L^{-1}), but was negligible in A1 (Figure 7, Table 7). Manganese was negligible (< 0.01 mg L^{-1}) along both A1 and A4 transects. Sulfate was also negligible (< 0.01 mg L^{-1}) along A1, but varied along the A4 transect, and was most concentrated (4.72 to 12.04 mg L^{-1}) from 0 m to 20 m downslope. Soil pore water within A1 in September 2018 had the highest concentration of NO_3^- (29.22 mg L^{-1}) observed at A1 throughout all four sampling campaigns. No precipitation events occurred during sampling in September 2018.

3.4. Isotopes of Nitrate and Water

A total of 62 soil pore water samples from within and downslope locations had sufficient NO_3^- concentrations (> 0.5 mg L^{-1}) to measure $\delta^{15}N$ and $\delta^{18}O$ of NO_3^- across all four sampling campaigns (Figure 8). $\delta^{15}N - NO_3^-$ at A1 and A4 downslope locations ranged from -0.6 ‰ to 9.0 ‰ and $\delta^{18}O - NO_3^-$ ranged from -10.5 ‰ to 4.1 ‰. Generally, higher $\delta^{18}O - NO_3^-$ values correspond to higher $\delta^{15}N - NO_3^-$ values at the downslope locations (Table 8). All samples collected from the seep downslope of A1 contained $\delta^{15}N - NO_3^-$ values close to 0 ‰ (-0.2 ‰ to 3.4 ‰) and $\delta^{18}O - NO_3^-$ ranged from to -9.8 ‰ to -0.1 ‰. Locations within A1 and A4 had $\delta^{15}N - NO_3^-$ that ranged from -13.8 ‰ to 9.6 ‰ and $\delta^{18}O - NO_3^-$ from -12.3 ‰ to 15.5 ‰. Soil pore water $\delta^{18}O$ ranged from -19.4 ‰ downslope of A4 in July 2018 to -13.6 ‰ between A1 and A4 in September 2017. $\delta^{15}N$ of leaf litter N collected from all five alder patches ranged from -2.8 ‰

to -0.2 ‰. $\delta^{15}N$ of total dissolved nitrogen (TDN) ranged from -11.3 ‰ to -0.9 ‰, and $\delta^{15}N$ of dissolved organic nitrogen (DON) ranged from -14.3 ‰ to -0.7 ‰ within A1 and A4 and -19.1 ‰ to -14.2 ‰ downslope of A1 and A4. $\delta^{15}N$ of SON ranged from 0.5 ‰ to 3.6 ‰ (n = 13). Oxygen and deuterium ($\delta^{18}O$ and δD) of water ranged from -19.4 ‰ to -12.2 ‰ and -132.2 ‰ to -102.1 ‰, respectively. A summary of NO_3^- and H_2O isotopic compositions are provided in Table 8 and Table 9, respectively.

4.0. DISCUSSION

4.1. Nitrate Sources

While previous studies conducted in continuous, polygonal permafrost areas without alders indicate that soil moisture is the dominant control on NO_3^- production (Arendt *et al., In Prep.*), no direct relationship (Figure 2; $r^2 = 0.001$) was observed between soil moisture and NO_3^- at the KG Hillslope. Although NO_3^- was generally elevated on the well-drained hillslope and absent on the poorly drained downslope, concentrations were further constrained by alder presence (soil pore water on the hillslope adjacent to and upslope of alders did not contain elevated NO_3^-). Therefore, while soil moisture likely plays a role in determining NO_3^- availability, our results indicate that alders are the dominant control on NO_3^- production in soil pore water on the KG Hillslope.

The coefficient of variability was calculated for Ca, Na, Cl^- and NO_3^- (Table 10) in order to directly compare the variability of each constituent across the landscape, where ratios closer to zero indicate less variation (Brown, 1998). Ca, Na, and Cl^- are all compounds that typically have low variability within the environment. High ratios of NO_3^- (> 1.0) and low ratios of Ca and Na

(< 1.0) indicate additional (biological) processes acting on NO_3^- production. Variability of Cl^- is likely influenced by weathering processes acting on the underlying bedrock on the hillslope.

The production of NO_3^- through nitrification is a microbially mediated process that produces predictable isotopic compositions through kinetic fractionation (Kendall & McDonnell, 1998). Based on the assumption that microbial nitrification utilizes two oxygen (O) atoms from water (H_2O) and one O atom from the atmosphere (O_2), the expected range of $\delta^{18}O - NO_3^-$ derived from microbial nitrification can be calculated using Equation 1:

$$\delta^{18}O - NO_3 = \frac{2}{3}(\delta^{18}O - H_2O) + \frac{1}{3}(\delta^{18}O - O_2) \quad \text{(Eq. 1)}$$

where atmospheric $\delta^{18}O\text{-}O_2$ is +23.5 ‰ (Kendall & McDonnell, 1998). However, other studies suggest that $\delta^{18}O\text{-}NO_3^-$ should more closely represent $\delta^{18}O\text{-}H_2O$ (Boshers, et al., 2019). We determined the range of $\delta^{18}O\text{-}NO_3^-$ derived by microbial nitrification to include both possibilities, as shown in Figure 8.

Because minimal fractionation takes place during N_2 fixation, NO_3^- produced by mineralization and nitrification of organic matter derived from fixation (alder leaf litter) should have $\delta^{15}N\text{-}NO_3^-$ in the range of 0.0 ± 5.0 ‰ (Kendall & McDonnell, 1998). Lighter sources of $\delta^{15}N\text{-}NO_3^-$ (< -5.0 ‰) are likely derived from more reduced sources of DON in the soil (Table 8). The concentration of DON was calculated as the difference between TDN-N and NO_3^--N (Equation 2), and the range of $\delta^{15}N$-DON was derived using Equation 3.

$$[DON] = [TDN] - [NO_3] \quad \text{(Eq. 2)}$$

$$\delta^{15}N_{DON} = \frac{(\delta^{15}N_{TDN} * [TDN]) - (\delta^{15}N_{NO3} * [NO3])}{[DON]} \quad \text{(Eq. 3)}$$

Of 29 samples from locations within alder patches, 21 fall in the range of $\delta^{15}N\text{-}NO_3^-$ = 0.0 ± 5.0 ‰, indicating that NO_3^- is likely produced primarily through mineralization and nitrification of leaf litter and organic matter derived from alders. Light $\delta^{15}N\text{-}NO_3^-$ (< -5.0 ‰) values are likely representative of NO_3^- derived from nitrification of DON produced by plant types other than alder. Atmospheric NO_3^- values of $\delta^{15}N$ range from ~ -15 ‰ to ~ +15 ‰ and $\delta^{18}O$ ranging from ~ +60 ‰ to ~ +94 ‰ (values obtained using the widely employed denitrifier method; Granger & Wankel, 2016). Isotopic signatures from 27 locations within alders (out of 29 total) plot within the expected range of $\delta^{18}O$ - NO_3^- of microbially derived NO_3^- (Figure 8), indicating that the soil pore water NO_3^- is a product of microbial mineralization and nitrification and not atmospheric deposition.

4.2. Precipitation

Previous studies have linked nutrient flushing occurring with rainfall events (Bechtold *et al*., 2003; Baldwin & Mitchell, 2000), and several studies have proposed that soil NO_3^- inputs from leaf litter during dry periods are mobilized at wet-season onset (Yamashita *et al*., 2010; Bernal *et al.*, 2003). In particular, Vink *et* al., (2007) found that in a forested catchment, inorganic N was accumulated within soil and leaf litter during dry periods and was subsequently flushed into headwater streams during precipitation events – an initial pulse in NO_3^- in soil pore water quickly declined following increased precipitation and discharge. The dynamic temporal variability of NO_3^- observed within and downslope of A1 associated with precipitation events in July and September of 2017 provides evidence that a similar model of NO_3^- accumulation and subsequent mobilization occurs on the KG Hillslope. A ‘pulse-like’ signal of elevated soil pore water NO_3^- was observed within and downslope of A1 (Figure 4) that corresponded to a precipitation event which occurred overnight between July 17 – 18, 2017. This event is reflected

in the $\delta^{18}O$ - NO_3^- of two samples collected from within A1 during this time period, where enriched values of $\delta^{18}O$ (> 10.0 ‰; Figure 8) may indicate a minor influence by atmospheric deposition of NO_3^-.

Rainfall occurred during sampling on all three days of the September 2017 campaign (9/14/17 through 9/16/17; direct observation; Western Regional Climate Center, 2017). This precipitation is reflected in the isotopic composition of water samples collected in September 2017, which had an average $\delta^{18}O$ value of -15.6 ± 0.83 ‰; around ~1 ‰ more enriched than water samples collected in July 2017, July 2018, and September 18 (Table 9; Figure 9). During July 2018 (July 22-27) and September 2018 (September 21-22) campaigns, weather conditions were much drier (no recorded precipitation events) and NO_3^- concentrations showed little variation with no daily pattern, ranging from 4.09 mg L^{-1} to 4.94 mg L^{-1} downslope of A1 over the five days in July 2018 and from 0.02 mg L^{-1} to 0.12 mg L^{-1} over two days in September 2018. While the precipitation events in July 2017 and September 2017 did appear to mobilize NO_3^- within A1 down-gradient and onto the KG Toe Slope, this effect was only observed within the first 10-30 m downslope of A1 (Figure 4), indicating the presence of additional controls acting on NO_3^- transport at the KG Hillslope.

The isotopic ratios of $\delta^{18}O$ to δD both on the KG Hillslope (r^2 = 0.92; Figure 10) and Toe Slope (r^2 = 0.81; Figure 10) indicate that evaporation was negligible during sampling (Figure 10). Water on the KG Hillslope was heavier in $\delta^{18}O$ composition (-15.62 ± 0.86 ‰) than water on the KG Toe Slope (-16.56 ± 0.48 ‰; Figure 10). There are two scenarios that explain these isotopic deviations. First, water on the KG Hillslope is influenced by isotopically heavier rainwater whereas water on the KG Toe Slope is influenced by a mixture of rainwater and isotopically lighter active layer ice melt (Craig, 1961). Second, water drains from the KG

Hillslope onto the KG Toe Slope and becomes depleted in $\delta^{18}O$ relative to the hillslope as residence time increases due to a lack of evaporation and vertical drainage (Kendall & McDonnell, 1998). It is likely that these each of these scenarios are in part influencing the isotopic composition of water (and subsequently NO_3^-) at the KG field site.

4.3. Redox

The increase in soil moisture, Fe^{2+}, and Mn, and decrease in NO_3^- along the A4 transect and decrease in NO_3^- along the A1 transect in July 2018 and September 2018 indicate a transition from an oxic environment towards a more sub-oxic environment as the slope breaks (Figure 6b; Tables 5 and 6). The lack of variation in SO_4^{-2} across these transects indicates conditions that are not reducing enough for sulfate reduction or methanogenesis (Jakobsen & Postma, 1999). The oxic environment on the well-drained KG Hillslope is ideal for NO_3^- production while sub oxic environment of the poorly drained KG Toe Slope is ideal for the reduction or denitrification of NO_3^-.

In a reducing environment, enrichment of $\delta^{15}N$ and $\delta^{18}O$ occurs during the process of microbial denitrification (Böttcher *et al.,* 1990). In freshwater systems, this enrichment is typically expressed as a 1:1 ($\delta^{18}O$/ $\delta^{15}N$) relationship, though many systems have trajectories greater or less than 1 (Boshers *et al.,* 2019). Deviations from a trajectory of 1 may be a result of nitrification and/or annamox (anaerobic ammonium oxidation) that produces NO_3^- concurrently during denitrification in anoxic conditions (Granger & Wankel, 2016). The downslope locations follow a similar trend of enrichment in $\delta^{15}N$ and $\delta^{18}O$ with an apparent regression slope of 0.84 (Figure 8), suggesting denitrification occurring on the KG Toe Slope.

Callahan *et al.* (2017) described hillslope alders as 'hotspots' for NO_3^- inputs into streams at the hillslope scale, and Harms & Jones (2012) observed greater NO_3^- export in soils with

increased active layer thickness. These predictions are consistent with the elevated NO_3^- concentrations within and directly downslope of each alder patch. The prevailing sub-oxic conditions downslope of A1 and A4 likely prevent NO_3^- production, indicating that elevated NO_3^- concentrations observed at these locations was produced within the alder patches and flushed downslope. However, mobility of NO_3^- beyond the first 20-30 m downslope of A1 and A4 was not observed, likely due to denitrification occurring in the sub-oxic conditions.

Similarly, a study by Harms & Ludwig (2016) predicted that saturated soils and reducing conditions may buffer N export to downslope ecosystems. Thus, while hillslopes dominated by alder will likely increase NO_3^- availability with shrubification, sub-oxic to reducing zones and soil saturation occurring at downslope locations may serve as buffers to down gradient mobility of NO_3^- through microbial denitrification. Defining the role of topographically controlled redox environments on nutrient cycling in permafrost environments will be beneficial for understanding the likelihood of NO_3^- mobilization to streams and subsequent transport down-gradient within N-limited landscapes.

4.4. Nitrate Variability

Results from this study are consistent with previous studies that reported elevated concentrations of NO_3^- in soils underlying alders in northwest Alaska and in the Swiss Alps (Rhoades *et al.*, 2001 and Bühlmann *et al.*, 2016, respectively). However to our knowledge, this study is the first to specifically identify the spatial (Figures 3 & 5) and temporal (Figure 4) heterogeneity of soil pore water NO_3^- within a permafrost landscape dominated by alder patches, and to address the possible controls on this variability. Findings from this study illuminate a level of complexity in nutrient cycling that is not well understood and provides a framework for future research in this topic.

4.4.1. Spatial Trends

Alders have been found to indirectly (through nitrification of leaf litter and woody plant material) supply NO_3^- to soil in N limited environments (Hiltbrunner *et al.*, 2014). On the KG Hillslope, NO_3^- was notably concentrated within alder patches and highly variable from one patch to another, ranging from a low of 0.30 mg L^{-1} in A4 to a high of 58.61 mg L^{-1} in A3 (15.50 ± 24.42 mg L^{-1}; Table 4) during our initial sampling campaign, similar to a study in the Swiss Alps where NO_3^--N was as high as 15.6 mg L^- (Buḧlmann *et al.*, 2016). Four of the five alder patches (all but A4) on the KG Hillslope had elevated NO_3^- (> 1.0 mg L^{-1}) at the 'within' locations during the Phase 1 (July 2017) synoptic sampling campaign, while no upslope locations and only one downslope location (Figure 3) had NO_3^- > 1.0 mg L^{-1}.

NO_3^- was concentrated within or directly downslope of A1 and A4 in all Phase 2 field campaigns (September 2017, July 2018, and September 2018; Figures 4, 5, and 6). In September 2017, NO_3^- and Fe_{Total} concentrations within A1 were not significantly different ($p = 0.28$) than downslope of A1, perhaps due to precipitation and subsequent NO_3^- flushing response on the hillslope. In July and September 2018, both NO_3^- and Fe_{Total} concentrations within A1 and A4 differed significantly ($p < 0.001$) from concentrations downslope of A1 and A4 (Figures 5-7; Table 7).

4.4.2. Temporal Trends

The greatest temporal variability in NO_3^- was observed in A1 during July and September 2017 during or following precipitation events (Figure 4). In July 2017, NO_3^- progressed from negligible concentrations within A1 preceding rainfall, to ~ 9 mg L^{-1} in the days following rainfall. In September of 2017, there was notable temporal variability with an observed daily increase in NO_3^- downslope of A1 during our three-day time series (Figure 4; Table 4), ranging

from 1.46 mg L^{-1} to 5.49 mg L^{-1}. Daily variation in NO_3^- concentrations was not observed during dry sampling periods; and the notable day-to-day changes in soil pore water NO_3^- appear to be driven primarily by precipitation events.

Seasonal variability is likely driven by microbial activity. In September 2017 and September 2018, a subset (8 of 14) of samples from within alder patches locations had light $\delta^{15}N\text{-}NO_3^-$ (< -5.0 ‰). This NO_3^- was likely derived from nitrification of DON (Figure 8) not associated with alder material. One explanation for the mixing of NO_3^- produced from alder material and NO_3^- produced from more reduced sources of DON may be a result of lower fixation rates late in the growing season, as productivity increases with soil temperature (Nadelhoffer *et al.*, 1990). Cooler temperatures in September may result in slower degradation of leaf litter and subsequent nitrification of mixed sources, yet high nutrient pools and increased rates of nutrient cycling have been observed late in the growing season prior to senescence (Mack *et al.*, 2004; Buckeridge *et al.*, 2009). Seasonal isotopic trends across all four campaigns of this study are compared in Figure 11, where the denitrification signature is seen most clearly in July 2017 (slope = 1.21) and July 2018 (slope = 0.79) and least clearly in September 2017 (slope = 0.30) and September 2018 (slope = 0.50), and supports the hypothesis that cooler temperatures late in the growing season slow microbial degradation.

5.0. SUMMARY

5.1. Spatial and Temporal Variability of Nitrate

Over the 2017 and 2018 growing seasons, significant spatiotemporal variability of soil pore water NO_3^- concentrations were observed at the permafrost KG Hillslope. Spatial variability existed within individual patches as well as from one patch to another. These spatial differences

encompassed both changes in the distribution of NO_3^- within patches and changes in the magnitude of NO_3^- present in the landscape over time. Temporally, we observed dynamic daily variability in NO_3^- correlated with precipitation events at locations within and downslope of an alder patch. On the KG Hillslope, NO_3^- likely accumulates in the soil below alders as litter decomposes, and gets mobilized down-gradient with the onset of rainfall. Evidence for this concept was observed after the isolated precipitation event in July 2017 where NO_3^- concentrations were elevated both within and downslope of one alder patch, and again in September 2017 where NO_3^- concentrations were elevated downslope but not within the same alder patch. These spatial variations associated with rainfall indicate a 'flushing' down gradient of previously accumulated soil NO_3^- from within the alder patch and highlight the capacity for NO_3^- to be mobilized across landscapes. Overall, NO_3^- had greater daily variability during wet conditions than during dry conditions (September 2017 vs. September 2018, respectively), suggesting that short term variation is driven by more by precipitation than seasonality.

5.2. Topography and Redox

The geomorphic characteristics (gradient, presence and depth of permafrost) of the KG Hillslope and KG Toe Slope catalyze a transition from oxidizing conditions on the KG Hillslope to sub-oxic conditions on the KG Toe Slope. Isotope analysis of water (oxygen and deuterium) revealed negligible evaporation occurring at the KG location throughout sampling. Dual oxygen and nitrogen isotope analyses provides insight to biochemical N processes that occur along the transition. We calculated the expected $\delta^{15}N\text{-}NO_3^-$ range of NO_3^- produced by microbial nitrification and compared our soil pore water nitrogen and oxygen isotope compositions to determine the most likely processes responsible for N fixation at the KG field site. Our findings suggest microbial mineralization and nitrification of organic N inputs derived through N_2

fixation by alders was likely the dominant source of NO_3^- production within A1 and A4 in July and that some organic matter from non-alder plant types was nitrified in September. Enrichment of $\delta^{15}N$ and $\delta^{18}O$ indicate the presence of denitrification at downslope locations, which may buffer N exports to streams and water bodies. Downslope of alder patches, denitrification related to sub-oxic conditions prevents soil pore water NO_3^- production and constrains the geographical extent of NO_3^- flushing effects induced by rainfall events. Variation in $\delta^{15}N$ and $\delta^{18}O$ (more enriched during July sampling campaigns than September; Figure 11) at locations downslope of alders indicate that seasonal variability of NO_3^- is driven by microbial activity, while short term (daily) variation is driven by precipitation events.

5.3. Future Research

While this study observed high spatial and temporal variability of NO_3^- in relation to alder shrubs and topographic controls in permafrost landscapes, future efforts should be made to better constrain the unique and complex characteristics of N cycling in the Arctic. Studies to further identify processes controlling the transport and fate of N in permafrost landscapes should include widespread, comprehensive investigations of N sources, total N input, organic carbon, microbial community function, and C:N relationships. For example, negligible NH_4^+ throughout the KG sampling locations suggests that nitrification is the main fate of NH_4^+ (Burger & Jackson, 2003), but the rates of mineralization have not been directly measured here. Future research should also emphasize the importance of characterizing N cycling to better constrain how storage and release of C will shift with climate warming in the Arctic. Long-term impacts of NO_3^- on vegetation, permafrost degradation, and interstitial water chemistry in wet downslope permafrost landscapes also require further studies. Lastly, identification of microbial communities in the

sub-oxic reducing environment downslope will lend insights towards the fate of NO_3^-, whether it is assimilated by plants or reduced to N_2 or nitrous oxide gas.

The dynamic variability of NO_3^- across the KG Hillslope demonstrates the importance of improving the representation of N cycle processes in ESMs. Including N and C ecological interactions in these models will decrease the uncertainty associated with forecasting atmospheric CO_2 concentrations in a warming climate (Thornton *et al.*, 2009) and bolster the predictive power of future models. Although plant functional types (PFTs) are included in ESMs currently, processes such as N-fixation remain underrepresented in these classifications (Wullschleger *et al.*, 2014). This study has shown the importance of incorporating such processes through representation of N-fixing shrubs in ESMs.

6.0. CONCLUSION

Understanding the relationships that exist between alders, topography, permafrost, and NO_3^- availability is more complicated and more spatially and temporally variable than previously realized. However, we have determined that the fixation of N within alder nodules and associated microbial plant material degradation is likely the dominant process responsible for elevated soil pore water NO_3^- in proximity to alder stands. In N-limited environments such as the Arctic, excess NO_3^- has the potential to propagate vegetation growth (Hiltbrunner *et* al., 2014; Weintraub & Schimel, 2003; Myers-Smith *et al*., 2011) and impact streams and other water bodies via wide-scale hydrologic exports.

Nitrate present in soil under alder shrubs is mobilized downslope during rainfall events, however redox environments driven by hillslope topography are important factors in buffering the spatial extent of NO_3^- mobility across permafrost landscapes. The degree of NO_3^- variability

observed over short timescales (days) and distances (tens of meters) are not well documented outside this study. These findings have implications for the anticipated nutrient responses associated with the projected expansion of shrub vegetation in the Arctic and demonstrate the importance of incorporating factors such as topography, redox conditions, and vegetation in watershed scale studies. Along with permafrost thaw (Harms & Jones, 2012) and changes in soil moisture distribution (Arendt *et al., In Prep*), the expansion of N-fixing shrubs across tundra landscapes is a dominant mechanism that could greatly increase NO_3^- availability in the Arctic. This study demonstrates that to fully understand the impact of shrubification on NO_3^- production and export and accurately represent these dynamics in Earth System Models, scientists need to consider plant functional types, topographic and hydrologic gradients, and the presence of geochemical reducing zones that may affect NO_3^- fate and transport.

7.0. TABLES

Table 1: Ammonium concentrations measured in September 2017, July 2017, and September 2019. Values < 0.02 mg L^{-1} are not reported. Black horizontal lines separate sampling campaigns.

Date	*Chemical Parameter (mg L^{-1})*	*n*	*max*	*min*	*mean*	*std*
July-17	NH_4^+	1	0.08	0.08	-	-
Sept-17	NH_4^+	2	0.29	0.03	0.16	0.18
July-18	NH_4^+	13	0.08	0.02	0.04	0.02

Table 2: *In situ* chemical parameters measured during each sampling campaign. No measurements were collected in September 2018. Black horizontal lines separate sampling campaigns.

Date	*Chemical parameter*	*n*	*min*	*max*	*mean*	*std*
17-Jul	Dissolved Oxygen (mg L^{-1})	45	1.93	7.98	4.71	1.72
	pH	48	4.97	7.34	5.76	0.54
	Conductivity (µS cm^{-1})	-	-	-	-	-
17-Sep	Dissolved Oxygen (mg L^{-1})	3	3.86	7.04	4.97	1.79
	pH	20	4.74	6.42	5.47	0.44
	Conductivity (µS cm^{-1})	-	-	-	-	-
18-Jul	Dissolved Oxygen (mg L^{-1})	114	1.34	6.76	3.54	1.15
	pH	114	3.77	9.97	5.41	0.67
	Conductivity (µS cm^{-1})	114	0.02	0.16	0.07	0.04

Table 3: Soil depth (cm) and soil moisture (%) measured in July and September (2017) and July (2018). Location indicates the alder patches from which measurements were derived. 'Upslope' and 'Within' locations have been combined and are referred to as 'Hillslope'. Black horizontal lines separate sampling campaigns.

Date	*Parameter*	*Location*		*n*	*max*	*min*	*mean*	*std*
Jul-17	Depth (cm)	A1-A5	Hillslope	3	38.3	32.7	35.2	2.9
			Downslope	5	33	25.5	29.4	3.0
	Moisture (%)		Hillslope	19	67.7	4.3	28.5	23.8
			Downslope	8	83.9	8.9	55.9	20.9
Sep-17	Depth (cm)	A1/A4	Hillslope	9	66.0	43.6	45.7	21.7
			Downslope	5	66.7	48.8	56.5	5.4
	Moisture (%)		Hillslope	6	56.1	17.1	28.4	14.2
			Downslope	-	-	-	-	-
Jul-18	Depth (cm)	A1/A4	Hillslope	12	56	29.2	36.6	7.3
			Downslope	24	76.2	35.2	53.3	12.1
	Moisture (%)		Hillslope	7	57.6	16.2	36.7	14.9
			Downslope	18	82.7	19.2	51.0	22.6

Table 4: Ranges of NO_3^- concentrations of soil pore water from alder patch sampling locations (A1 through A5) collected during July and September 2017. The black horizontal line separates sampling campaigns.

Date	*Chemical Parameter (mg L^{-1})*	*Location*		*n*	*max*	*min*	*mean*	*std*
Jul-17	NO_3^-	A1-A5	Upslope	5	0.64	0.03	0.11	0.25
			Within	5	58.61	0.30	15.50	24.42
			Downslope	5	0.26	<0.01	0.10	0.11
Sep-17	NO_3^-	A1	Within	6	2.4	0.23	0.83	0.90
			Downslope	6	5.49	3.86	4.94	0.93
		A4	Within	2	11.41	6.18	8.79	3.70
			Downslope	2	0.01	<0.01	<0.01	<0.01
		Hillslope	Between A1/A4	4	0.01	<0.01	<0.01	<0.01

Table 5: NO_3^- and Fe_{Total} summary (2017). P-values less than 0.05 are significant. Outside alder refers to locations upslope and downslope of alder patches. Fan refers to the middle and road transects on the KG Toe Slope. The black horizontal line separates sampling campaigns.

Date	*Chemical Parameter (mg L^{-1})*	*Location*		*n*	*mean*	*std*	*P-value*
Jul-17	NO_3^-	A1/A4	Within alder	5	15.50	24.42	.004
			Outside alder	10	0.17	0.21	
Sep-17	NO_3^-	A1/A4	Within	8	2.79	4.04	0.28
			Downslope	8	1.90	2.57	
		Hillslope	Within + Downslope	16	2.35	3.30	0.01
		Fan	Middle Transect	3	<0.01	<0.01	
	Fe_{Total}	A1/A4	Within	8	0.52	0.15	0.88
			Downslope	8	0.87	1.23	
		Hillslope	Within + Downslope	16	0.69	0.87	< 0.001
		Fan	Middle Transect	3	2.40	1.08	

Table 6: July 23-27, 2018. Chemical parameters and constituents (Sample mean and standard deviation). Samples starting with P indicate Pits dug along the A1 transect. Concentrations without a reported standard deviation are single values.

Sample ID	*NO_3^- (mg L^-)*	*St. Dev. NO_3^-*	*Mn (mg L^-)*	*St. Dev. Mn*	*Fe^{2+} (mg L^-)*	*St. Dev Fe^{2+}*	*SO_4^{2-} (mg L^-)*	*St. Dev SO_4^{2-}*
A1_DS_0	4.57	0.35	0.02	0.02	0.47	0.02	0.33	0.13
A1_DS_10	0.02	0.01	0.00	0.00	0.58	<0.01	0.39	0.25
A1_DS_20	0.43	0.10	0.01	0.00	0.31	0.06	1.77	0.22
A1_DS_30	0.03	0.02	0.00	0.00	0.69	0.06	0.65	0.25
A1_DS_40	0.07	0.04	0.00	0.00	0.77	0.01	0.42	0.24
A1_DS_50	0.02	0.01	0.01	0.00	0.67	<0.01	0.39	0.26
A1_DS_Seep	0.65	0.11	0.00	0.00	<0.01	<0.01	1.27	0.04
A1_WI_Down	0.82	0.98	0.01	0.00	0.22	0.06	0.27	0.12
A1_WI_Mid	0.51	0.42	0.01	0.00	0.26	0.11	0.51	0.31
A1_WI_Up	6.52	1.24	0.01	0.00	0.70	0.17	0.44	0.19
A4_DS_0	2.08	0.96	0.00	0.00	0.03	0.02	4.50	0.40
A4_DS_10	0.04	0.06	0.03	0.02	0.73	0.90	0.66	0.20
A4_DS_20	0.03	0.04	0.05	0.01	5.21	3.05	0.52	0.23
A4_DS_30	0.02	0.02	0.32	0.05	1.99	1.96	0.62	0.23
A4_DS_40	0.03	0.03	0.12	0.02	1.00	1.05	1.11	0.61
A4_DS_50	0.03	0.03	0.06	0.09	1.87	-	0.55	0.15
A4_WI_Down	2.50	0.45	0.01	0.00	0.2	0.17	0.59	0.49
A4_WI_Mid	0.70	0.48	0.01	0.00	0.32	0.03	0.53	0.43
A4_WI_Up	5.73	-	0.02	-	0.46	-	1.83	-
Between A1/A4	0.15	0.09	0.01	0.01	0.36	0.09	0.78	0.35
P1_20	3.57	0.67	0.01	0.01	0.44	-	1.40	0.21
P1_40	8.01	0.25	0.00	0.00	0.22	-	1.83	0.27
P1_60	8.32	1.64	0.01	0.00	0.15	-	5.23	0.46
P2_20	0.03	0.01	0.00	0.00	0.64	-	0.54	0.22
P2_40	0.03	0.02	0.01	0.00	0.15	-	3.41	0.43
P3_20	6.52	2.01	0.00	0.00	0.11	-	0.35	0.26
P3_40	7.59	2.03	0.01	0.00	0.53	-	0.31	0.09

Table 7: NO_3^- and Fe_{Total} summary (2018). P-values less than 0.05 are significant. The black horizontal line separates sampling campaigns.

Date	*Chemical Parameter* (mg L^{-1})	*Location*		*n*	*max*	*min*	*mean*	*std*	*P-value*
18-Jul	NO_3^-	A1	A1 Within	19	7.96	0.17	3.03	2.76	<0.001
			A1 Downslope	25	0.57	0.01	0.12	0.17	
		A4	A4 Within	16	3.16	0.04	1.65	1.06	<0.001
			A4 Downslope	25	0.14	<0.01	0.03	0.03	
		A1 & A4	Within	35	-	-	2.40	2.24	<0.001
			Downslope	50	-	-	0.07	0.13	
	Fe_{Total}	A1	A1 Within	19	0.94	0.08	0.40	0.25	0.08
			A1 Downslope	25	0.71	0.20	0.54	0.15	
		A4	A4 Within	16	0.52	0.04	0.22	0.14	<0.001
			A4 Downslope	25	11.36	0.78	5.65	3.59	
		A1 & A4	Within	35	-	-	0.32	0.23	<0.001
			Downslope	50	-	-	3.09	3.60	
18-Sep	NO_3^-	A1	A1 Within	4	17.73	0.58	5.72	8.08	0.002
			A1 Downslope	10	0.12	0.01	0.05	0.37	
		A4	A4 Within	4	8.44	3.21	4.63	2.55	0.002
			A4 Downslope	10	0.05	0.02	0.03	0.01	
		A1 & A4	Within	8	-	-	5.18	5.73	<0.001
			Downslope	20	-	-	0.04	0.03	
	Fe_{Total}	A1	A1 Within	4	0.68	0.15	0.40	0.27	0.14
			A1 Downslope	10	1.93	0.19	0.82	5.25	
		A4	A4 Within	4	0.11	0.05	0.08	0.03	0.002
			A4 Downslope	10	17.07	0.88	5.31	5.25	
		A1 & A4	Within	8	-	-	0.24	0.25	<0.001
			Downslope	20	-	-	3.07	4.30	

Table 8: Oxygen and nitrogen isotopic compositions from soil pore water nitrate. July 2017 through September 2018.

Isotope (‰)	*Location*	*n*	*max*	*min*	*mean*	*std*
$\delta^{18}O_{NO3-}$	Within	29	15.5	-12.3	-3.9	6.1
$\delta^{15}N_{NO3-}$			9.6	-13.8	-3.2	4.9
$\delta^{15}N_{leaf}$		5	-0.2	-2.8	-0.9	0.5
$\delta^{18}O_{NO3-}$	Downslope	26	4.1	-10.5	-6.1	3.1
$\delta^{15}N_{NO3-}$			9.0	-0.6	1.9	2.0
$\delta^{15}N_{H20}$	All locations	61	-13.6	-19.4	-16.4	1.06
$\delta^{15}N_{SON}$		13	3.6	0.5	2.0	0.9
$\delta^{15}N_{TDN}$		15	-2.6	-11.3	-5.9	3.0
$\delta^{15}N_{DON}$		12	-8.0	-19.1	-12.7	3.0

Table 9: Oxygen isotopic composition from soil pore water. July 2017 through September 2018. Black horizontal lines separate sampling campaigns.

Date	*Isotope (‰)*	*n*	*min*	*max*	*mean*	*std*
17-Jul	$\delta^{18}O$	48	-17.3	-15.6	-16.5	0.4
17-Sep	$\delta^{18}O$	28	-17.0	-13.6	-15.6	0.8
17-Jul	$\delta^{18}O$	116	-19.4	-14.4	-16.7	0.9
18-Sep	$\delta^{18}O$	80	-18.4	-12.3	-16.2	1.0

Table 10: Coefficient of variability ratio for calcium, sodium, chloride, and nitrate on hillslope and downslope locations. July 2017 through September 2018. Black horizontal lines separate sampling campaigns.

Date	*Location*	*Ca*	*Na*	*Cl^-*	*NO_3^-*
All	Hillslope	0.69	0.43	1.40	1.89
	Downslope	0.88	0.27	1.24	2.08
Jul-17	Hillslope	0.41	0.29	1.22	2.02
	Downslope	0.77	0.35	1.18	1.17
	All Locations	0.90	0.34	1.35	3.29
Sep-17	Hillslope	0.46	0.14	0.55	1.45
	Downslope	0.38	0.14	0.67	2.11
	All Locations	0.46	0.33	0.93	2.03
Jul-18	Hillslope	0.51	0.27	0.43	1.06
	Downslope	0.71	0.20	0.30	1.97
	All Locations	0.901	0.28	0.40	1.56
Sep-18	Hillslope	0.85	0.48	1.01	1.39
	Downslope	0.89	0.22	0.25	1.97
	All Locations	1.02	0.49	1.09	2.35

8.0. FIGURES

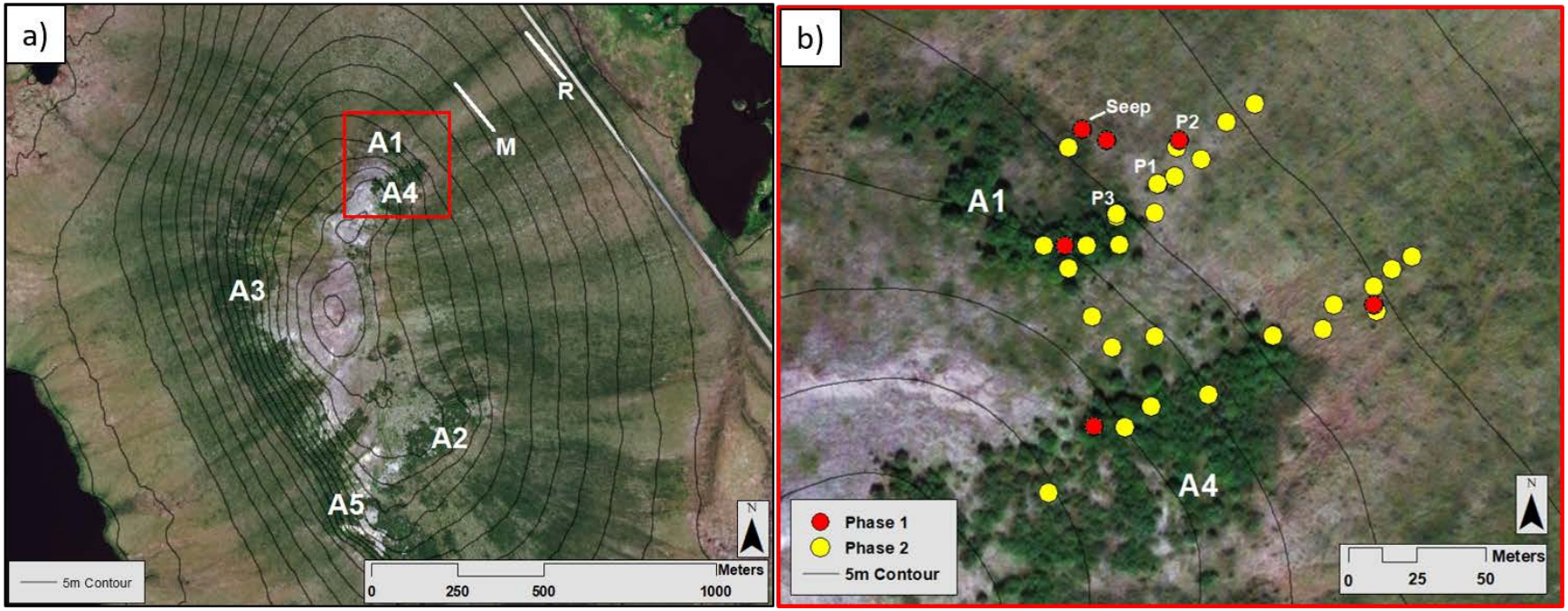

Figure 1: Kougarok Field Site and sampling locations, located 64 miles inland from the town of Nome on the Seward Peninsula, AK. a) Phase 1 alder patch sampling locations (A1-A5). White lines represent Middle (M) and Road (R) sampling transects. b) Phase 2 sampling locations; corresponds to the red box in Figure 1a. Phase 1 locations are denoted with red dots. Yellow dots indicate additional locations sampled during Phase 2 (September 2017, July 2018, and September 2018). P1, P2, and P3 indicate Pit locations dug in July 2018. Sampling locations in part b are not to scale.

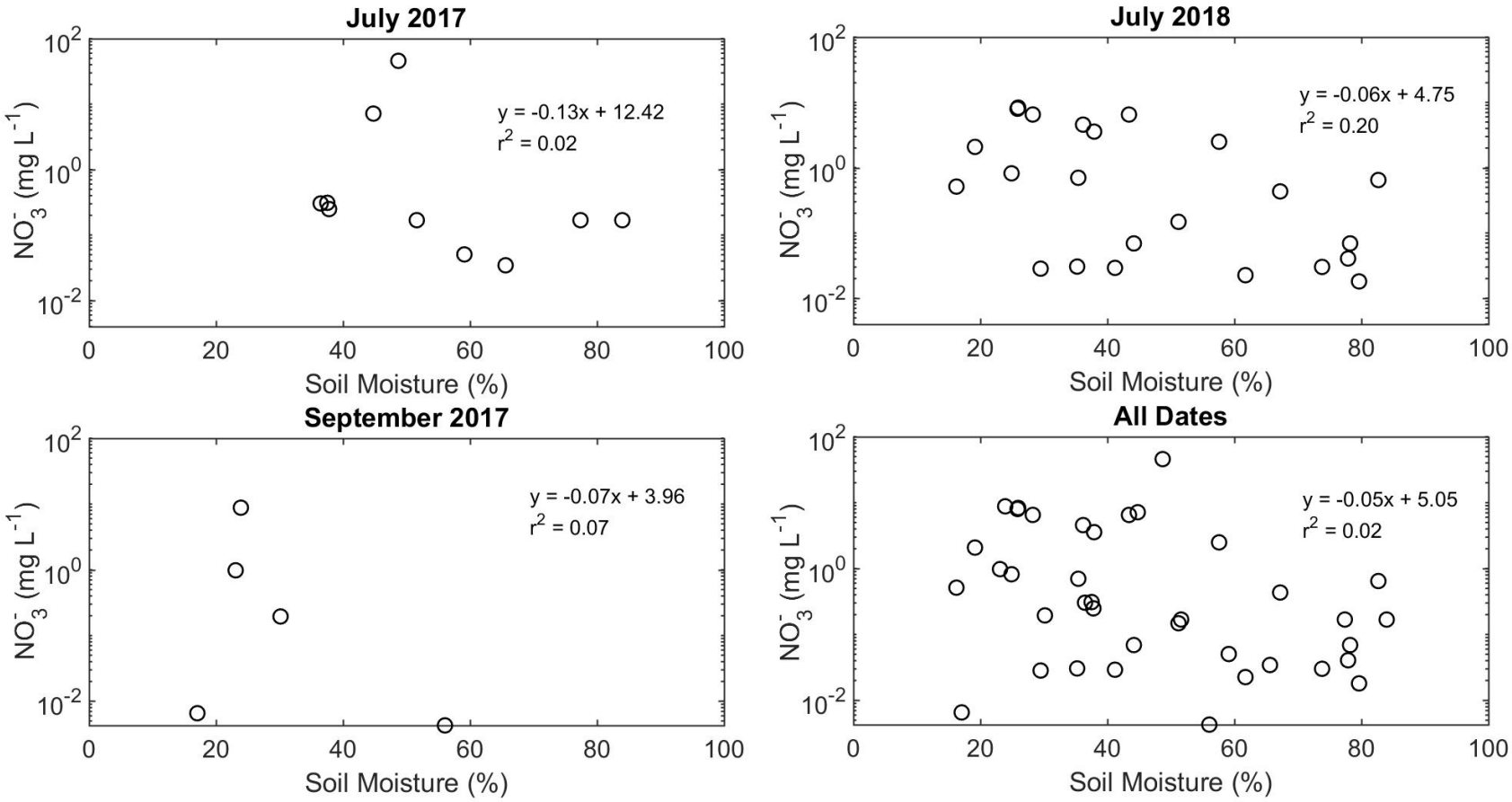

Figure 2: Soil moisture versus NO_3^- from July 2017, July 2018, September 2018, and all three seasons. No direct relationship was observed between soil pore water NO_3^- and soil moisture content.

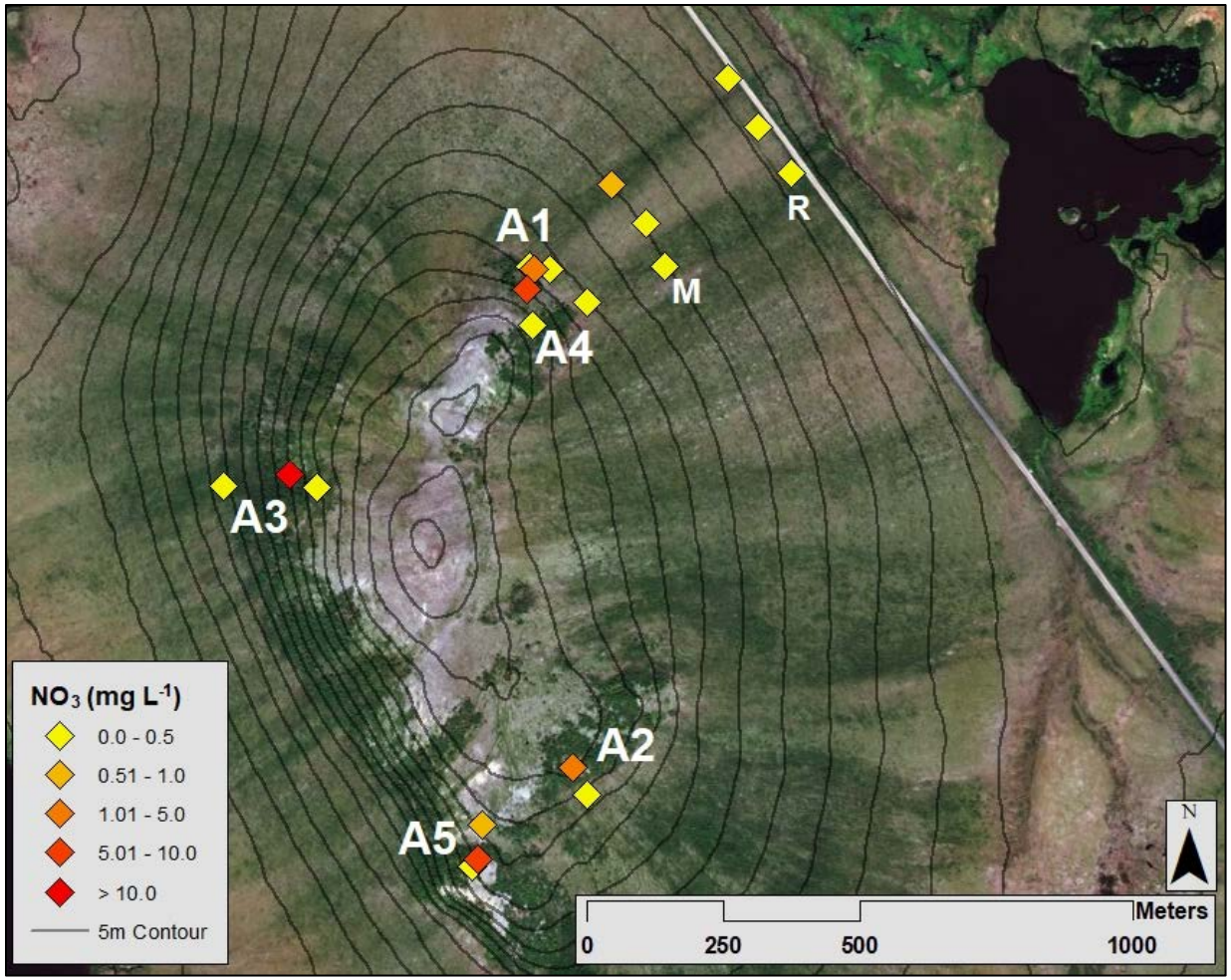

Figure 3: Map of mean NO_3^- concentrations from the July 2017 Phase 1 sampling locations. Diamonds represent NO_3^- concentrations at locations upslope, within, and downslope of all alder patches and Middle/Road transects, where yellow diamonds indicate low concentrations and red diamonds indicate high concentrations (see Key for ranges).

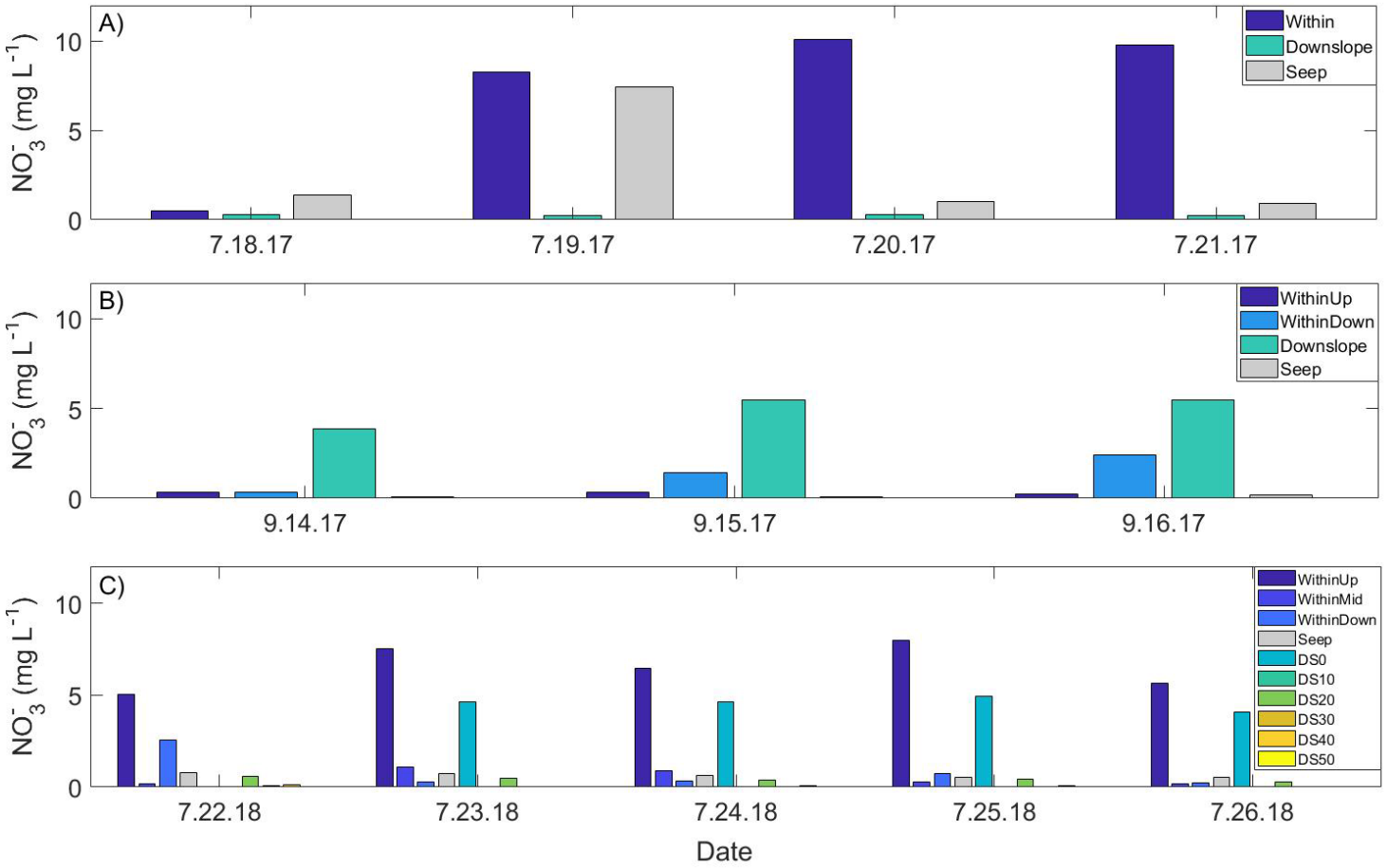

Figure 4: Soil pore water NO_3^- time series plots from Alder Patch 1 (A1). A) July 2017 daily NO_3^- concentrations from locations within and downslope of A1. 'Seep' denotes a seep in the ground located downslope of A1. B) September 2017 daily NO_3^- concentrations in A1. Locations within A1 were further discretized into two locations (WithinUp, WithinDown). C) September 2018 daily NO_3^- concentrations at A1 transect locations. WithinUp, WithinMid, and WithinDown refer to locations within A1, and "DS#" refers to the distance in meters along a 50 m transect downslope of A1. Days marked with an asterisk (*) indicate precipitation events.

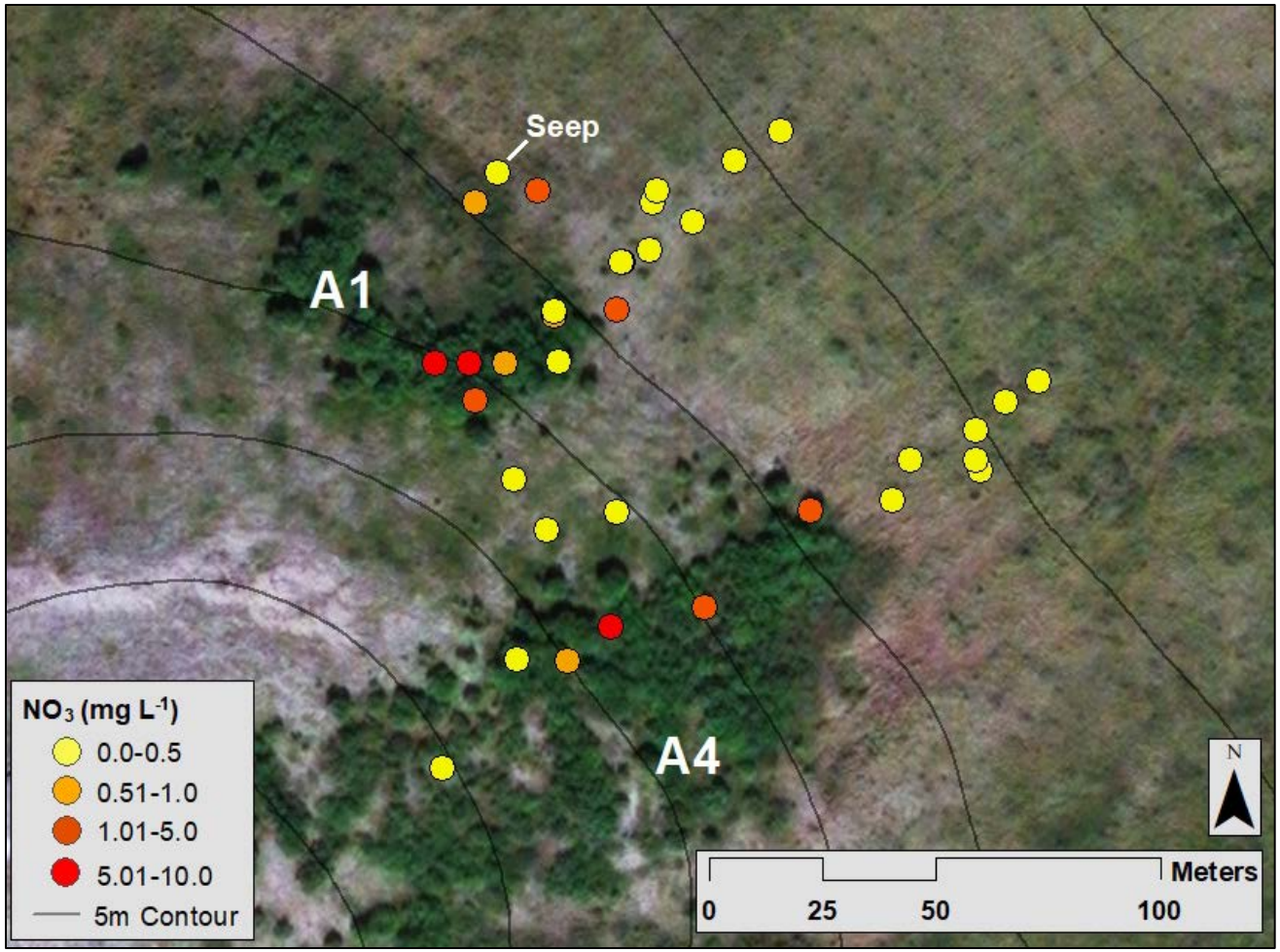

Figure 5: Mean soil pore water NO_3^- concentrations from A1 and A4 during Phase 2 (September 2017, July 2018, and September 2018), where yellow circles indicate low concentrations and red circles indicate high concentrations (see Key for ranges). Note that the NO_3^- ranges provided in the Key for Figure 4 are different than the NO_3^- ranges provided in Figure 2.

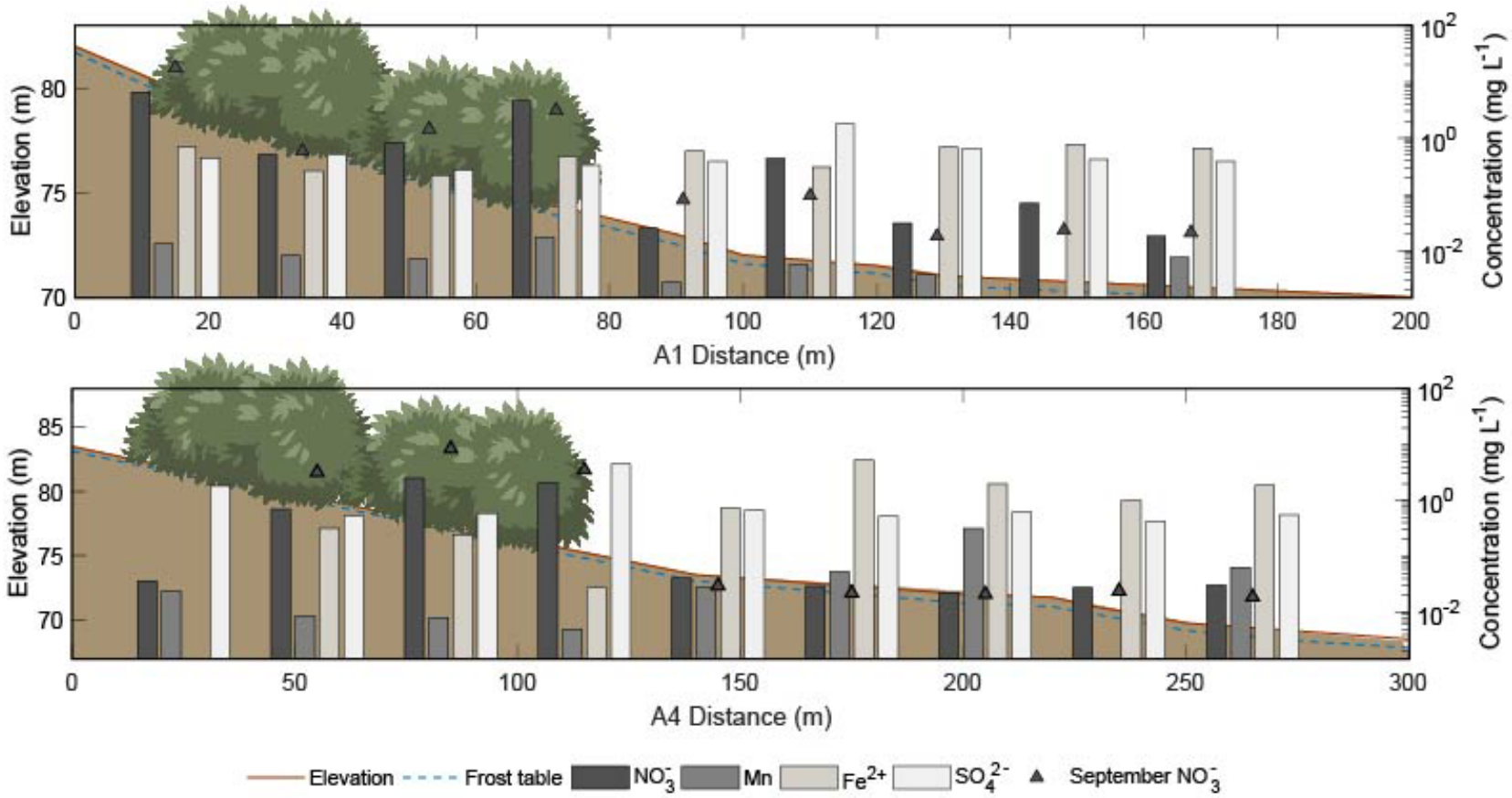

Figure 6: Elevation profiles and chemical concentrations along A1 and A4 transects during July and September (2018) sampling. Note that the elevation scale is different for A1 and A4. Depth to frozen soil or bedrock is depicted by the blue dashed line. Redox species: nitrate (NO_3^-), manganese (Mn), iron (Fe^{2+}), and sulfate (SO_4^{2-}) are plotted along the secondary y-axis. September 2018 NO_3^- concentrations are depicted by dark gray triangles.

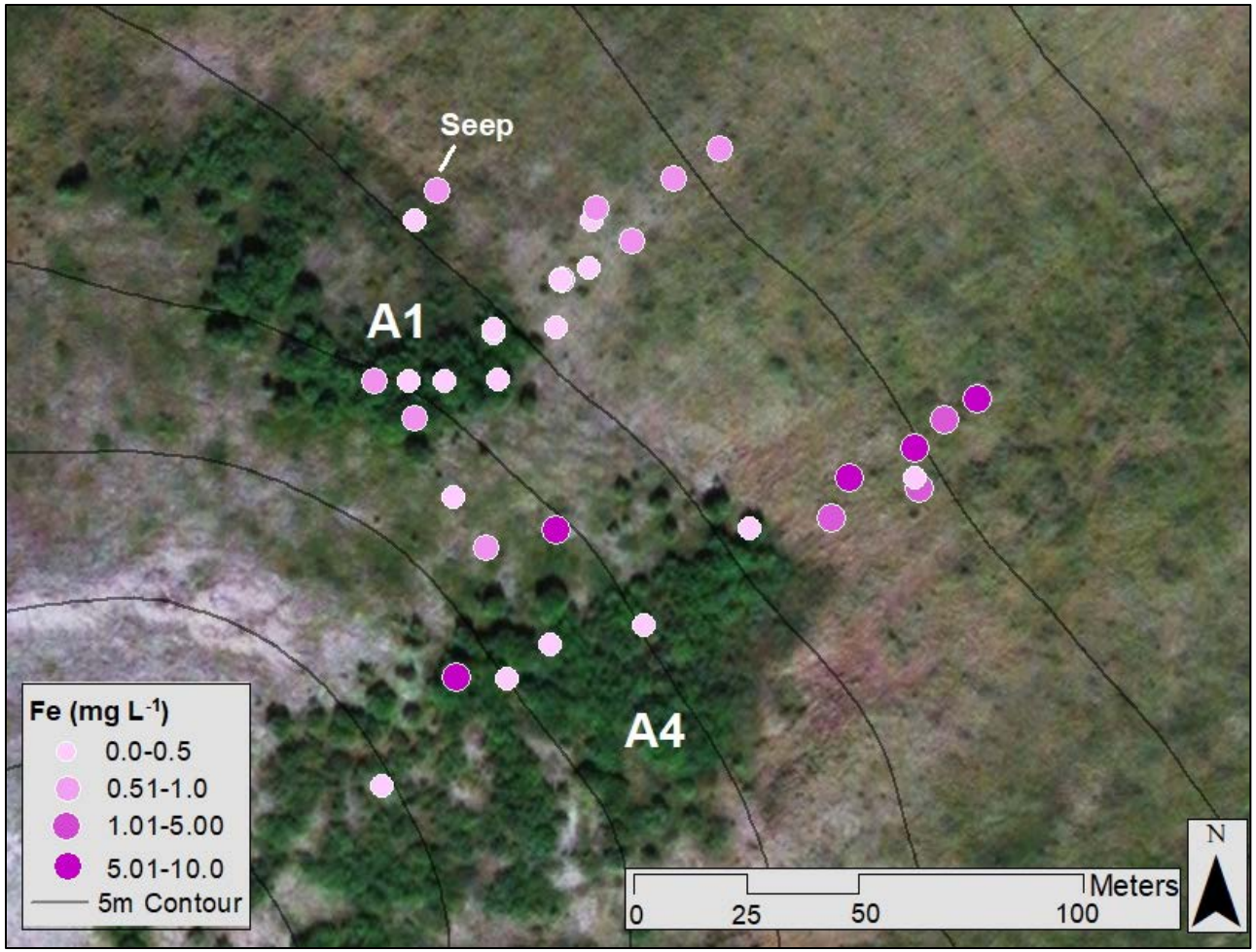

Figure 7: Soil pore water total iron (Fe_{Total}) concentrations from A1 and A4 during Phase 2 (July 2018), where light purple circles correspond to low concentrations and dark purple circles correspond to high concentrations.

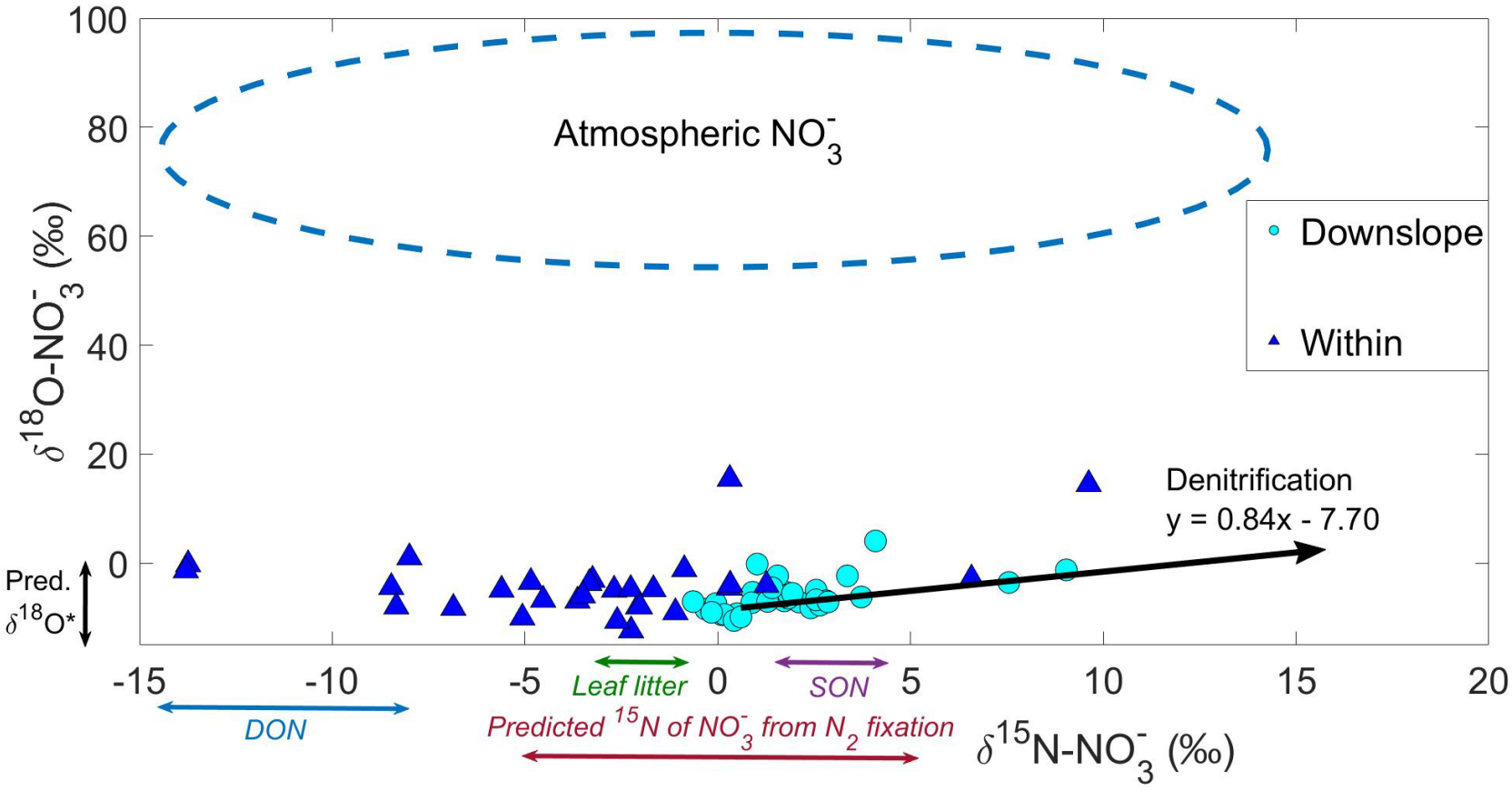

Figure 8: Oxygen ($\delta^{18}O$) versus nitrogen ($\delta^{15}N$) isotopes of soil pore water NO_3^-. Light blue triangles represent samples from within alder patches and dark blue circles represent samples from downslope of alder patches. The denitrification process is denoted by the black arrow inside the plot (y = 0.84x - 7.70). The black double arrow (Pred. $\delta^{18}O^*$) denotes the predicted range of $\delta^{18}O$ of NO_3^- produced by microbial nitrification (Equation 1). The red double arrow indicates mineralization and nitrification of organic matter derived from alder material (N-fixation; Kendall and McDonnell, 1998). $\delta^{15}N$ of N from leaf litter is shown by the green double arrow. The blue double arrow denotes the range of $\delta^{15}N$ of DON, and the purple double arrow indicates SON.

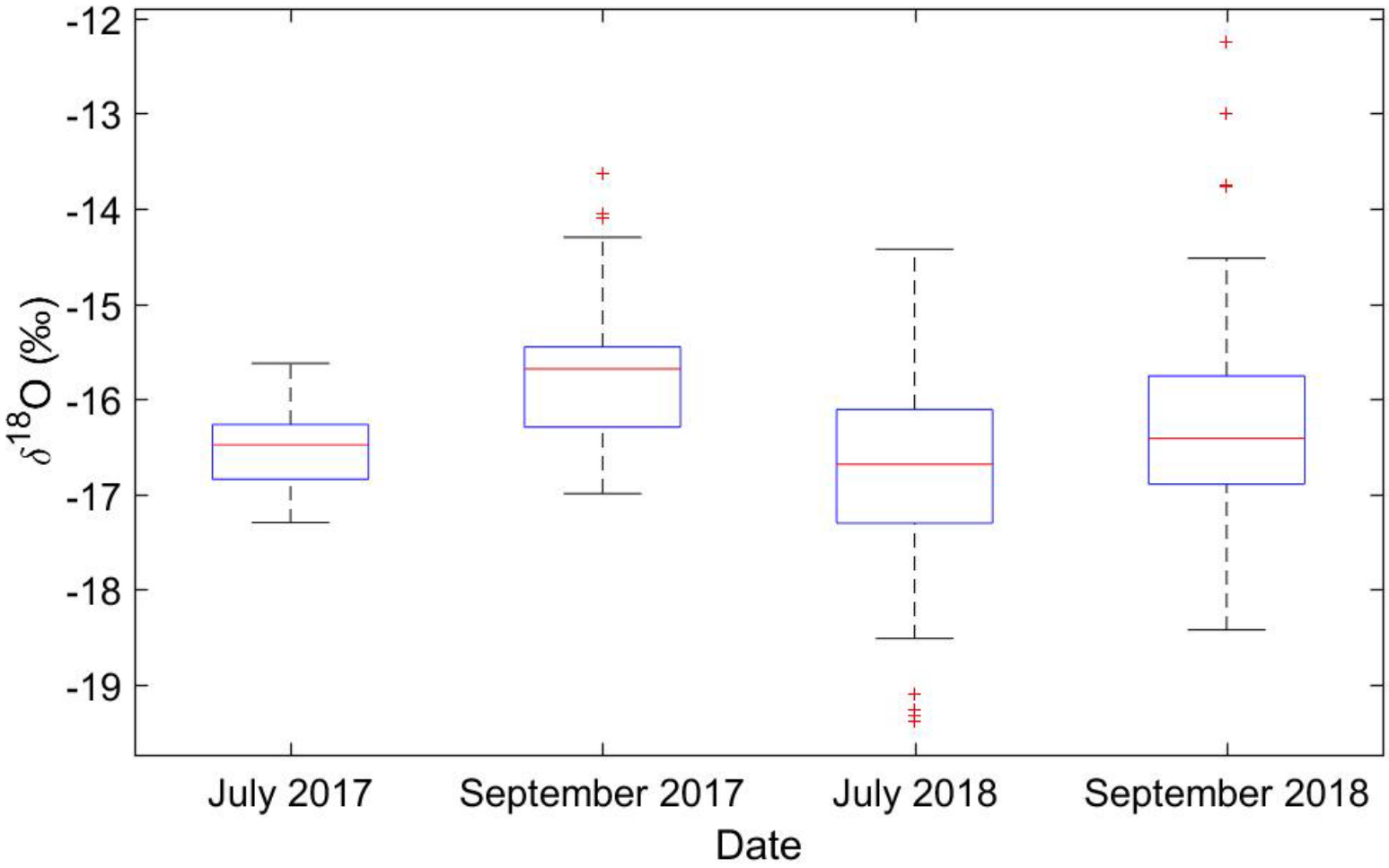

Figure 9: Oxygen isotopes ($\delta^{18}O$) of water during July 2017 and September of 2017 and 2018. The red line within each box represents the sample mean and red crosses indicate outliers.

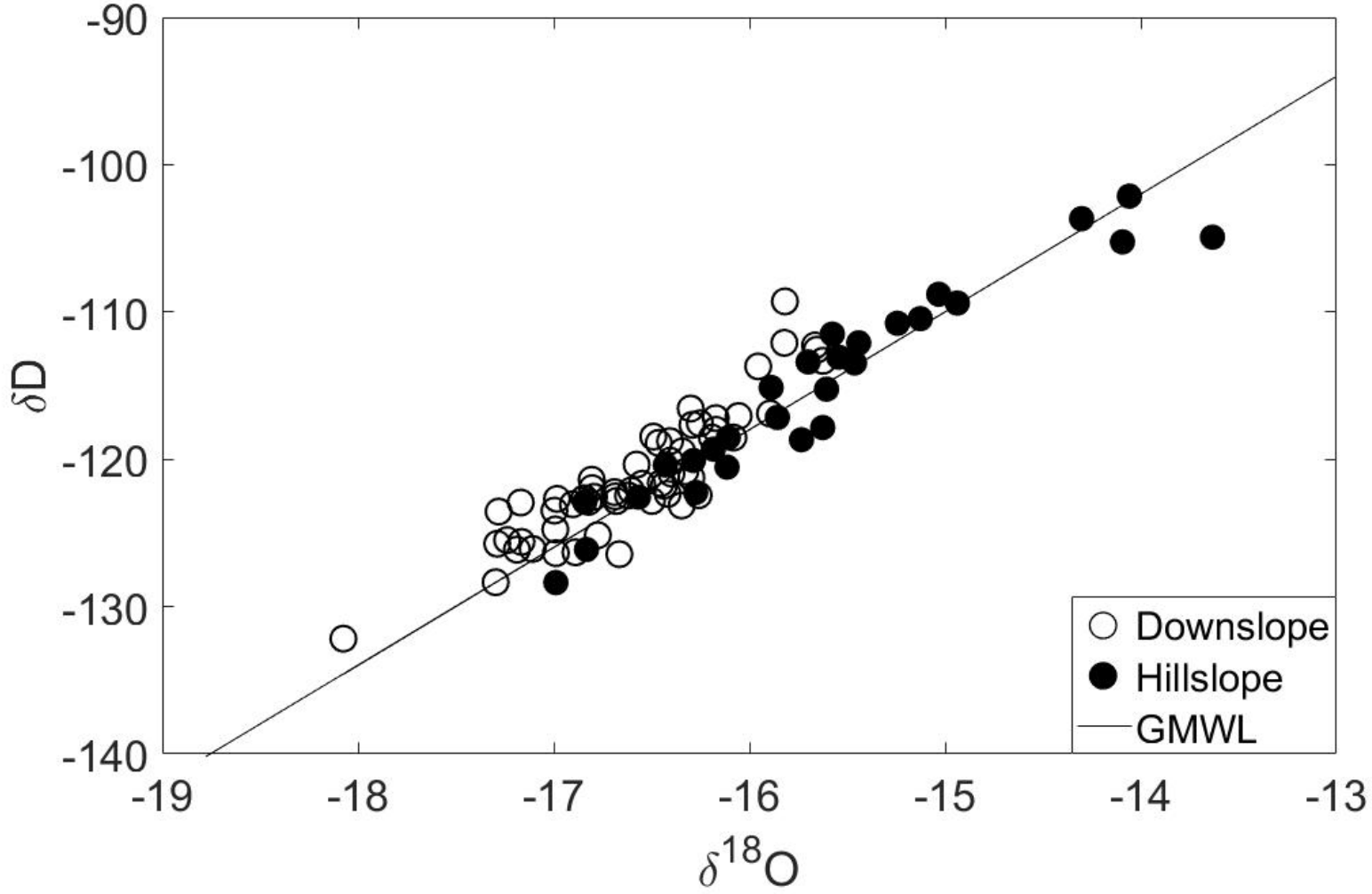

Figure 10: Soil pore water oxygen ($\delta^{18}O$) versus deuterium (δD) isotopes during July 2017 and September of 2017 and 2018. $\delta^{18}O$ and δD are plotted against the global meteoric water line (GMWL). Open circles represent downslope locations and closed circles represent hillslope locations.

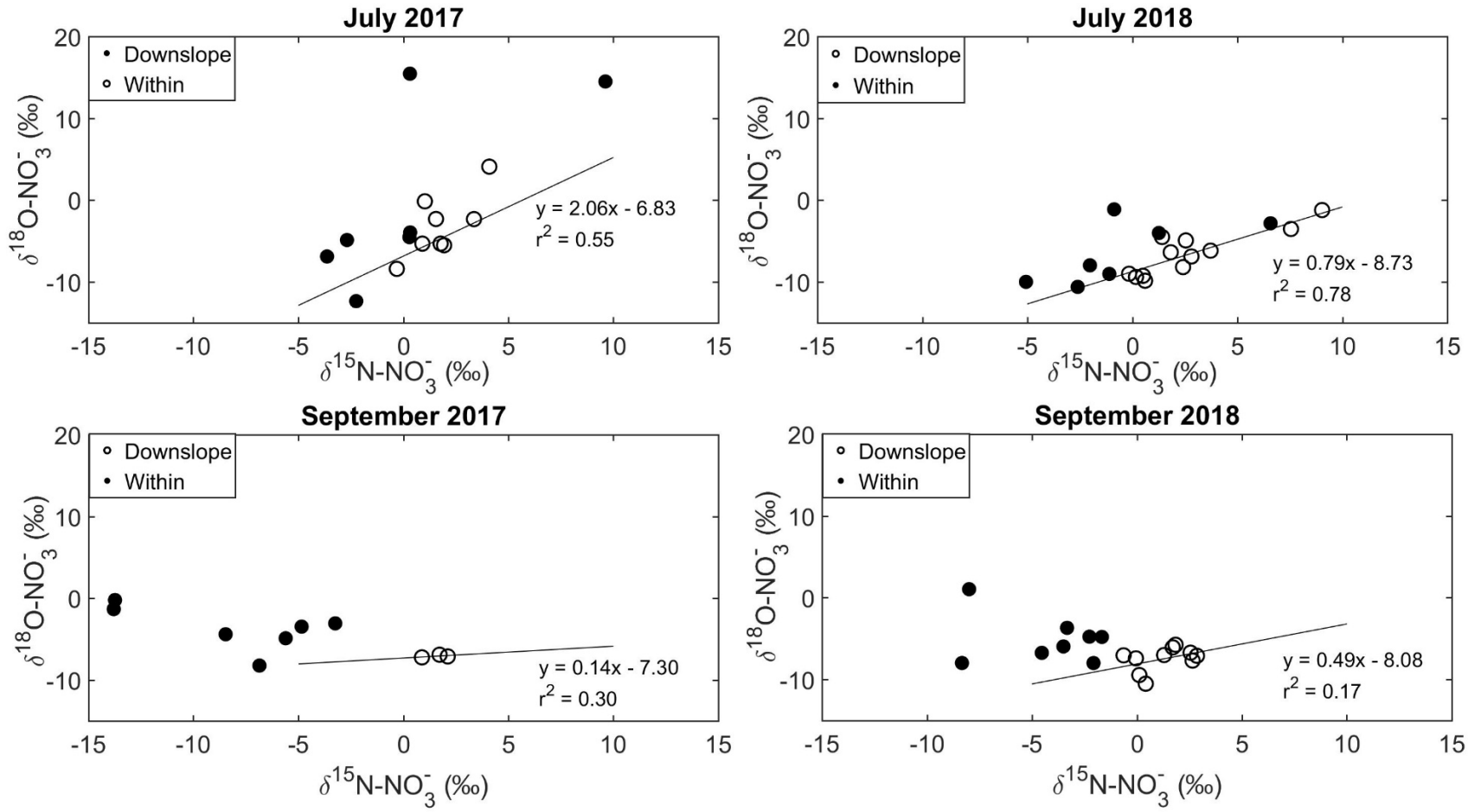

Figure 11: Oxygen ($\delta^{18}O$) versus nitrogen ($\delta^{15}N$) isotopes of soil pore water NO_3^- during July and September (2017 and 2018). Closed black circles represent samples from locations within alder patches and open black circles represent locations downslope of alder patches. Black trend lines and equations indicate enrichment of $\delta^{18}O$ and $\delta^{15}N$ of NO_3^- (indicating denitrification) occurring downslope during each season.

9.0 REFERENCES

Arendt, C. A., Heikoop, J. M., Newman, B. D., Wilson, C. J., Wainwright, H., Kumar, J., *et al*., (*In Prep*.) Increased Arctic nitrate related to permafrost thaw, landscape evolution, and soil drying.

Atchley, A. L., Coon, E. T., Painter, S. L., Harp, D. R., & Wilson, C. J. (2016). Influences and interactions of inundation, peat, and snow on active layer thickness. *Geophysical Research Letters*, *43*(10), 5116–5123. https://doi.org/10.1002/2016GL068550

Baldwin, D. S., & Mitchell, A. M. (2000). The effects of drying and re-flooding on the sediment and soil nutrient dynamics of lowland river-floodplain systems: A synthesis. *Regulated Rivers-Research & Management*, *16*(5), 457–467. https://doi.org/10.1002/1099-1646(200009/10)16:5<457::AID-RRR597>3.3.CO;2-2

Barnes, R. T., Williams, M. W., Parman, J. N., Hill, K., & Caine, N. (2014). Thawing glacial and permafrost features contribute to nitrogen export from Green Lakes Valley, Colorado Front Range, USA. *Biogeochemistry*, *117*(2), 413–430. https://doi.org/10.1007/s10533-013-9886-5

Bechtold, J. S., Edwards, R. T., & Naiman, R. J. (2003). Biotic versus hydrologic control over seasonal nitrate leaching in a floodplain forest. *Biogeochemistry*, *63*(1), 53–72. https://doi.org/10.1023/A:1023350127042

Bense, V. F., Ferguson, G., & Kooi, H. (2009). Evolution of shallow groundwater flow systems in areas of degrading permafrost. *Geophysical Research Letters; Washington*, *36*(22). http://dx.doi.org.prox.lib.ncsu.edu/10.1029/2009GL039225

Bernal, S., Butturini, A., Nin, E., Sabater, F., & Sabater, S. (2003). Leaf Litter Dynamics and Nitrous Oxide Emission in a Mediterranean Riparian Forest. *Journal of Environmental Quality*, *32*(1), 191–197. https://doi.org/10.2134/jeq2003.1910

Boike, J., Juszak, I., Lange, S., Chadburn, S., Burke, E., Overduin, P. P., & Westermann, S. (2018). A 20-year record (1998–2017) of permafrost, active layer and meteorological conditions at a high Arctic permafrost research site (Bayelva, Spitsbergen). *Earth System Science Data; Katlenburg-Lindau*, *10*(1), 355–390. http://dx.doi.org.prox.lib.ncsu.edu/10.5194/essd-10-355-2018

Boshers, D. S., Granger, J., Tobias, C. R., Böhlke, J. K., & Smith, R. L. (2019). Constraining the oxygen isotopic composition of nitrate produced by nitrification. *Environmental Science & Technology*, *53*(3), 1206–1216. https://doi.org/10.1021/acs.est.8b03386

Böttcher, J., Strebel, O., Voerkelius, S., & Schmidt, H.-L. (1990). Using isotope fractionation of nitrate-nitrogen and nitrate-oxygen for evaluation of microbial denitrification in a sandy aquifer. *Journal of Hydrology*, *114*(3), 413–424. https://doi.org/10.1016/0022-1694(90)90068-9

Brown, C. E. (1998). Coefficient of Variation. In C. E. Brown (Ed.), *Applied Multivariate Statistics in Geohydrology and Related Sciences* (pp. 155–157). Berlin, Heidelberg: Springer Berlin Heidelberg. https://doi.org/10.1007/978-3-642-80328-4_13

Buckeridge, K. M., Zufelt, E., Chu, H., & Grogan, P. (2010). Soil nitrogen cycling rates in low arctic shrub tundra are enhanced by litter feedbacks. *Plant and Soil; Dordrecht*, *330*(1–2), 407–421. http://dx.doi.org/10.1007/s11104-009-0214-8

Bühlmann, T., Hiltbrunner, E., & Körner, C. (2014). Alnus viridis expansion contributes to excess reactive nitrogen release, reduces biodiversity and constrains forest succession in the Alps. *Alpine Botany*, *124*(2), 187–191. https://doi.org/10.1007/s00035-014-0134-y

Bühlmann, T., Körner, C., & Hiltbrunner, E. (2016). Shrub Expansion of Alnus viridis Drives Former Montane Grassland into Nitrogen Saturation. *Ecosystems*, *19*(6), 968–985. https://doi.org/10.1007/s10021-016-9979-9

Burger, M., & Jackson, L. E. (2003). Microbial immobilization of ammonium and nitrate in relation to ammonification and nitrification rates in organic and conventional cropping systems. *Soil Biology and Biochemistry*, *35*(1), 29–36. https://doi.org/10.1016/S0038-0717(02)00233-X

Callahan, M. K., Whigham, D. F., Rains, M. C., Rains, K. C., King, R. S., Walker, C. M, *et al.* (2017).Nitrogen subsidies from hillslope alder stands to streamside wetlands and headwater streams, Kenai Peninsula, Alaska. *JAWRA Journal of the American Water Resources Association*, *53*(2), 478–492. https://doi.org/10.1111/1752-1688.12508

Casciotti, K. L., Sigman, D. M., Hastings, M. G., Böhlke, J. K., & Hilkert, A. (2002). Measurement of the oxygen isotopic composition of nitrate in seawater and freshwater using the denitrifier method. *Analytical Chemistry*, *74*(19), 4905–4912. https://doi.org/10.1021/ac020113w

Chapin, F. S., Mcguire, A. D., Randerson, J., Pielke, R., Baldocchi, D., Hobbie, S. E., *et al.* (2000). Arctic and boreal ecosystems of western North America as components of the climate system. *Global Change Biology*, *6*(S1), 211–223. https://doi.org/10.1046/j.1365-2486.2000.06022.x

Craig, H. (1961). Isotopic Variations in Meteoric Waters. *Science,133*(3465), 1702-1703. Retrieved from http://www.jstor.org.prox.lib.ncsu.edu/stable/1708089

Euskirchen, E. S., Bennett, A. P., Breen, A. L., Genet, H., Lindgren, M. A., Kurkowski, T. A., *et al.* (2016). Consequences of changes in vegetation and snow cover for climate feedbacks in Alaska and northwest Canada. *Environmental Research Letters*, *11*(10), 105003. https://doi.org/10.1088/1748-9326/11/10/105003

Granger, J., & Wankel, S. D., (2016). Isotopic overprinting of nitrification on denitrification as a ubiquitous and unifying feature of environmental nitrogen cycling. *Proceedings of the National Academy of Sciences*, 113 (42) E6391-E6400; DOI:10.1073/pnas.1601383113

Harms, T. K., & Jones, J. B. (2012). Thaw depth determines reaction and transport of inorganic nitrogen in valley bottom permafrost soils. *Global Change Biology*, *18*(9), 2958–2968. https://doi.org/10.1111/j.1365-2486.2012.02731.x

Harms, T. K., & Ludwig, S. M. (2016). Retention and removal of nitrogen and phosphorus in saturated soils of arctic hillslopes. *Biogeochemistry*, *127*(2), 291–304. https://doi.org/10.1007/s10533-016-0181-0

Heikoop, J. M., Throckmorton, H. M., Newman, B. D., Perkins, G. B., Iversen, C. M., Chowdhury, T. R., *et al*. (2015). Isotopic identification of soil and permafrost nitrate sources in an Arctic tundra ecosystem, *Journal of Geophysical Research Biogeoscience*, 120, 1000–1017. DOI: 10.1002/2014JG002883.

Helsel, D.R. & Hirsch, R.M. (2002). Statistical Methods in Water Resources Techniques of Water Resources Investigations, Book 4, Chapter A3. U.S. Geological Survey. pp. 118.

Hiltbrunner, E., Aerts, R., Bühlmann, T., Huss-Danell, K., Magnusson, B., Myrold, D. D., *et al.* (2014). Ecological consequences of the expansion of N2-fixing plants in cold biomes. *Oecologia*, *176*(1), 11–24. https://doi.org/10.1007/s00442-014-2991-x

Hinzman, L. D., Deal, C. J., McGuire, A. D., Mernild, S. H., Polyakov, I. V., & Walsh, J. E. (2013). Trajectory of the Arctic as an integrated system. *Ecological Applications*, *23*(8), 1837–1868. https://doi.org/10.1890/11-1498.1

Hovelsrud, G. K., Poppel, B., van Oort, B., & Reist, J. D. (2011). Arctic societies, cultures, and peoples in a changing cryosphere. *AMBIO*, *40*(1), 100–110. https://doi.org/10.1007/s13280-011-0219-4

Hugelius, G., Strauss, J., Zubrzycki, S., Harden, J. W., Schuur, E. a. G., Ping, C.-L., *et al.* (2014). Estimated stocks of circumpolar permafrost carbon with quantified uncertainty ranges and identified data gaps. *Biogeosciences*, *11*(23), 6573–6593. https://doi.org/10.5194/bg-11-6573-2014

Hurd, T. M., & Raynal, D. J. (2004). Comparison of nitrogen solute concentrations within alder (Alnus incana ssp. rugosa) and non-alder dominated wetlands. *Hydrological Processes*, *18*(14), 2681–2697. https://doi.org/10.1002/hyp.5575

Iversen, C. M., Sloan V. L., Sullivan P. F., Euskirchen E. S., McGuire, A., Norby, D. Richard J., *et al.* (2014). The unseen iceberg: plant roots in arctic tundra. *New Phytologist*, *205*(1), 34–58. https://doi.org/10.1111/nph.13003

Iversen, C., Breen, A., Salmon, V., Vander Stel, H., & Wullschleger, S. NGEE Arctic Plant Traits: Vegetation plot locations, ecotypes, and photos, Kougarok Road mile marker 64, Seward Peninsula, Alaska, 2016. Next Generation Ecosystem Experiments Arctic Data Collection, Oak Ridge National Laboratory, U.S. Department of Energy, Oak Ridge, Tennessee, USA. [2016].

Jakobsen, R., & Postma, D. (1999). Redox zoning, rates of sulfate reduction and interactions with Fe-reduction and methanogenesis in a shallow sandy aquifer, Rømø, Denmark. *Geochimica et Cosmochimica Acta*, *63*(1), 137 151. https://doi.org/10.1016/S0016-7037(98)00272-5

Kendall, C., & McDonnell, (1998). Isotope tracers in catchment hydrology (Eds.). Elsevier Science B.V., Amsterdam. pp. 519-576.

Keuper, F., Bodegom, P. M. van, Dorrepaal, E., Weedon, J. T., Hal, J. van, Logtestijn, R. S. P. van, & Aerts, R. (2012). A frozen feast: thawing permafrost increases plant-available nitrogen in subarctic peatlands. *Global Change Biology*, *18*(6), 1998–2007. https://doi.org/10.1111/j.1365-2486.2012.02663.x

Keuper, F., Dorrepaal, E., Bodegom, P. M. van, Logtestijn, R. van, Venhuizen, G., Hal, J. van, & Aerts, R. (2017). Experimentally increased nutrient availability at the permafrost thaw front selectively enhances biomass production of deep-rooting subarctic peatland species. *Global Change Biology*, *23*(10), 4257–4266. https://doi.org/10.1111/gcb.13804

Koch, J. C., Runkel, R. L., Striegl, R., & McKnight, D. M. (2013). Hydrologic controls on the transport and cycling of carbon and nitrogen in a boreal catchment underlain by continuous permafrost. *Journal of Geophysical Research: Biogeosciences*, *118*(2), 698–712. https://doi.org/10.1002/jgrg.20058

Mack, M. C., Schuur, E. A. G., Bret-Harte, M. S., Shaver, G. R., & Chapin, F. S. (2004). Ecosystem carbon storage in arctic tundra reduced by long-term nutrient fertilization. *Nature; London*, *431*(7007), 440–443. https://doi-org.prox.lib.ncsu.edu/10.1038/nature02887

Martin, P. D., Jenkins, J. L., Adams, F. J., Torre, M., Matz, A. C., Payer, D. C., *et al.*, (2008). Predicting Future Habitats of Arctic Alaska, *Report from the Wildlife Response to Environmental Arctic Change (WildREACH): Predicting Future Habitats of Arctic Alaska Workshop.* 142.

McClelland, J. W., Stieglitz, M., Pan, F., Holmes, R. M., & Peterson, B. J. (2007). Recent changes in nitrate and dissolved organic carbon export from the upper Kuparuk River, North Slope, Alaska: N and C export from the Kuparuk River. *Journal of Geophysical Research: Biogeosciences*, *112*(G4), https://doi.org/10.1029/2006JG000371

Minsley, B. J., Abraham, J. D., Smith, B. D., Cannia, J. C., Voss, C. I., Jorgenson, M. T., *et al.* (2012). Airborne electromagnetic imaging of discontinuous permafrost. *Geophysical Research Letters; Washington*, *39*(2). http://dx.doi.org.prox.lib.ncsu.edu/10.1029/2011GL050079

Mitchell, J. S., & Ruess, R. W. (2009). N2 fixing alder (Alnus viridis spp. fruticosa) effects on soil properties across a secondary successional chronosequence in interior Alaska. *Biogeochemistry*, *95*(2), 215–229. https://doi.org/10.1007/s10533-009-9332-x

Myers-Smith, I. H., Forbes, B. C., Wilmking, M., Hallinger, M., Lantz, T., Blok, D, *et al.* (2011). Shrub expansion in tundra ecosystems: dynamics, impacts and research priorities. *Environmental Research Letters*, *6*(4), 045509. https://doi.org/10.1088/1748-9326/6/4/045509

Nadelhoffer, K. J., Giblin, A. E., Shaver, G. R. & Laundre, J. A. (1990). Effects of temperature and substrate quality on element mineralization in six arctic soils. *Ecology* 72, 242–253

O'donnell, J. A., & Jones, J. B. (2006). Nitrogen retention in the riparian zone of catchments underlain by discontinuous permafrost. *Freshwater Biology*, *51*(5), 854–864. https://doi.org/10.1111/j.1365-2427.2006.01535.x

Ogawa, A., Shibata, H., Suzuki, K., Mitchell, M. J., & Ikegami, Y. (2006). Relationship of topography to surface water chemistry with particular focus on nitrogen and organic carbon solutes within a forested watershed in Hokkaido, Japan. *Hydrological Processes*, *20*(2), 251–265. https://doi.org/10.1002/hyp.5901

Rhoades, C., Óskarsson, H., Binkley, & D., Stottlemyer, R. (2001). Alder (Alnus crispa) effects on soils in ecosystems of the Agashashok River valley, northwest Alaska. Ecoscience. 8. 89-95. 10.1080/11956860.2001.11682634.

Romanovsky, V. E., & Osterkamp, T. E. (2000). Effects of unfrozen water on heat and mass transport processes in the active layer and permafrost. *Permafrost and Periglacial Processes*, *11*(3), 219–239. https://doi.org/10.1002/1099-1530(200007/09)11:3<219::AID-PPP352>3.0.CO;2-7

Roy, S., Khasa, D. P., & Greer, C. W. (2007). Combining alders, frankiae, and mycorrhizae for the revegetation and remediation of contaminated ecosystems. *Canadian Journal of Botany; Ottawa*, *85*(3), 237–251.

Schädel, C., Bader, M. K., Schuur, E. A. G., Biasi, C., Bracho, R., Capek, P., *et al.* (2016). Potential carbon emissions dominated by carbon dioxide from thawed permafrost soils. *Nature Climate Change; London*, *6*(10), 950–953. http://dx.doi.org.prox.lib.ncsu.edu/10.1038/nclimate3054

Schuur, E. A. G., McGuire, A. D., Schädel, C., Grosse, G., Harden, J. W., Hayes, D. J., *et al.* (2015). Climate change and the permafrost carbon feedback. *Nature; London*, *520*(7546), 171–179.

Schuur, Edward A. G., Bockheim, J., Canadell, J. G., Euskirchen, E., Field, C. B., Goryachkin, S. V., *et al.* (2008). Vulnerability of permafrost carbon to climate change: Implications for the global carbon cycle. *BioScience*, *58*(8), 701–714. https://doi.org/10.1641/B580807

Sebestyen, S. D., Ross, S. D., Shanley, J. B., Elliott, E. M., Kendall, C., Campbell, J. L., *et al.* (2019). Unprocessed atmospheric nitrate in waters of the Northern Forest Region in the U.S. and Canada. *Environmental Science & Technology, 53* (7), 3620-3633. DOI: 10.1021/acs.est.9b01276

Seeberg-Elverfeldt, J., Schlüter, M., Feseker, T., & Kölling, M. (2005). Rhizon sampling of porewaters near the sediment-water interface of aquatic systems. *Limnology and Oceanography: Methods*, *3*(8), 361–371. https://doi.org/10.4319/lom.2005.3.361

Shaftel, R. S., King, R. S., & Back, J. A. (2012). Alder cover drives nitrogen availability in Kenai lowland headwater streams, Alaska. *Biogeochemistry*, *107*(1), 135–148. https://doi.org/10.1007/s10533-010-9541-3

Sharkhuu, N., & Sharkhuu, A. (2012). Effects of climate warming and vegetation cover on permafrost of Mongolia. In M. J. A. Werger & M. A. van Staalduinen (Eds.), *Eurasian Steppes. Ecological Problems and Livelihoods in a Changing World*, 445–472. Dordrecht: Springer Netherlands. https://doi.org/10.1007/978-94-007-3886-7_17

Shaver, G. R., & Chapin, F. S. (1980). Response to fertilization by various plant growth forms in an Alaskan tundra: Nutrient accumulation and growth. *Ecology*, *61*(3), 662–675. https://doi.org/10.2307/1937432

Sigman, D. M., Casciotti, K. L., Andreani, M., Barford, C., Galanter, M., & Böhlke, J. K. (2001). A bacterial method for the nitrogen isotopic analysis of nitrate in seawater and freshwater. *Analytical Chemistry*, *73*(17), 4145–4153. https://doi.org/10.1021/ac010088e

Stookey, L. L. (1970). Ferrozine-A new pectrophotometric reagent for iron. *Analytical Chemistry, 42*(7), 779-781 DOI: 10.1021/ac60289a016

Street, L. E., Burns, N. R., & Woodin, S. J. (2015). Slow recovery of High Arctic heath communities from nitrogen enrichment. *New Phytologist*, *206*(2), 682–695. https://doi.org/10.1111/nph.13265

Tape, K., Sturm, M., & Racine, C. (2006). The evidence for shrub expansion in Northern Alaska and the Pan-Arctic. *Global Change Biology*, *12*(4), 686–702. https://doi.org/10.1111/j.1365-2486.2006.01128.x

Thornton, P. E., Doney, S. C., Lindsay, K., Moore, J. K., Mahowald, N., Randerson, J. T., *et al.* (2009). Carbon-nitrogen interactions regulate climate-carbon cycle feedbacks: results from an atmosphere-ocean general circulation model. *Biogeosciences*, *6*(10), 2099–2120. https://doi.org/10.5194/bg-6-2099-2009

Throckmorton, H. M., Heikoop, J. M., Newman, B. D., Altmann, G. L., Conrad, M. S., Muss, J. D., *et al.*, (2015). Pathways and transformations of dissolved methane and dissolved inorganic carbon in Arctic tundra watersheds: Evidence from analysis of stable isotopes, *Global Biogeochemical Cycles*, 29, 1893–1910 doi: 10.1002/2014GB005044.

Vink, S., Ford, P. W., Bormans, M., Kelly, C., & Turley, C. (2007). Contrasting nutrient exports from a forested and an agricultural catchment in south-eastern Australia. *Biogeochemistry*, *84*(3), 247–264. https://doi.org/10.1007/s10533-007-9113-3

Vitousek, P. M., Aber, J. D., Howarth, R. W., Likens, G. E., Matson, P. A., Schindler, D. W., *et al.* (1997). Human alteration of the global nitrogen cycle: Sources and consequences. *Ecological Applications, 7*(3), 737–750. https://doi.org/10.1890/1051-0761(1997)007[0737:HAOTGN]2.0.CO;2

Walvoord, M. A., & Kurylyk, B. L. (2016). Hydrologic impacts of thawing permafrost—A Review. *Vadose Zone Journal*, *15*(6). https://doi.org/10.2136/vzj2016.01.0010

Walvoord, M. A., Voss, C. I., & Wellman, T. P. (2012). Influence of permafrost distribution on groundwater flow in the context of climate-driven permafrost thaw: Example from Yukon Flats Basin, Alaska, United States. *Water Resources Research*, *48*(7). https://doi.org/10.1029/2011WR011595

Weintraub, M. N., & Schimel, J. P. (2005). Nitrogen cycling and the spread of shrubs control changes in the carbon balance of Arctic tundra ecosystems. *BioScience*, *55*(5), 408–415. https://doi.org/10.1641/0006-3568(2005)055[0408:NCATSO]2.0.CO;2

Weintraub, M. N., & Schimel, J. P. (2003). Interactions between carbon and nitrogen mineralization and soil organic matter chemistry in Arctic tundra soils. *Ecosystems*, *6*(2), 0129–0143. https://doi.org/10.1007/s10021-002-0124-6

Western Regional Climate Center (2017). *RAWS USA Climate Archive*. Retrieved from: https://raws.dri.edu/cgi-bin/rawMAIN.pl?akAQTZ

Whigham, D. F., Walker, C. M., Maurer, J., King, R. S., Hauser, W., Baird, S., *et al.* (2017). Watershed influences on the structure and function of riparian wetlands associated with headwater streams - Kenai Peninsula, Alaska. *Science of the Total Environment*, *599*, 124–134. https://doi.org/10.1016/j.scitotenv.2017.03.290

Woo, M.-K., Kane, D. L., Carey, S. K., & Yang, D. (2008). Progress in permafrost hydrology in the new millennium. *Permafrost and Periglacial Processes*, *19*(2), 237–254. https://doi.org/10.1002/ppp.613

Wullschleger, S. D., Epstein, H. E., Box, E. O., Euskirchen, E. S., Goswami, S., Iversen, C. M., *et al.* (2014). Plant functional types in Earth system models: past experiences and future directions for application of dynamic vegetation models in high-latitude ecosystems. *Annals of Botany*, *114*(1), 1–16. https://doi.org/10.1093/aob/mcu077

Yamashita, N., Ohta, S., Sase, H., Luangjame, J., Visaratana, T., Kievuttinon, B., & Kanzaki, M. (2010). Seasonal and spatial variation of nitrogen dynamics in the litter and surface soil layers on a tropical dry evergreen forest slope. *Forest Ecology and Management*, *259*(8), 1502–1512. https://doi.org/10.1016/j.foreco.2010.01.026